Ion cyclotron (IC) oscillations excited by nonlinear waves propagating in collision-free auroral ionosphere

John Z. G. Ma[*1] and **J.-P. St.-Maurice** [2]

[1] California Institute of Integral Studies, San Francisco, CA, USA

[2] Department of Physics and Engineering Physics, University of Saskatchewan, Saskatchewan, Canada

We study ion cyclotron (IC) oscillations activated by a stochastic, strong space-charge electric wavefield **E** of nonlinear waves propagating auroral ionosphere. **E** is in a plane perpendicular to the ambient magnetic field **B**. The word "strong" means that (1) the conventional linear plasma wave model connected to a perturbed electric field is not suitable to be employed; (2) the $\mathbf{E} \times \mathbf{B}$ drift is comparable to (even higher than) the thermal speed of particles, and drive them away from the initial thermal equilibrium. A physical model is set up for a dense cluster of electron soliton trains with which a magnetic flux tube is teeming. Then, the collision-free Boltzmann equation is solved under the condition that **E** is temporally constant. With a nonzero initial guiding-center (GC) velocity, ions are found to follow a double-circle trajectory in velocity space with an IC oscillation frequency ω which shifts from the magnetic gyrofrequency $\Omega = eB/m_i$ (where e and m_i are the charge and mass of the singly ionized ions, respectively). Furthermore, the "constant" condition is relaxed by using a simple stochastic **E** which has 10-step random strengths in 10 different time intervals. The accommodation of ω (as well as other parameters) is illustrated in response to the **E** switches. At last, the work is generalized by using two random-number generators for the strength and time, respectively. In this case, ω can be shifted to several Ω values. This result is in good agreement with what FAST satellite measured in auroral field-aligned current regions.

1 Introduction

Electrostatic ion-cyclotron (IC) oscillation mode was firstly predicted by *Stix* (1957) in studying an infinitely long, cylindrically symmetric plasma column of finite density (n_0) at zero pressure immersed in a uniform axial magnetic field (B). He pointed out that when $ck \gg \omega_{UH}$ and $ck/\omega \gg \omega_{UH}/\Omega$ [where c is the speed of light, k the wave vector along B, ω the wave frequency, $\Omega = (1/c)eB/m_i$ the ion cyclotron frequency with (e, m_i) the charge and mass of the singly ionized ion, respectively, $\omega_{UH} = \sqrt{\omega_{pi}^2 + \Omega^2}$ the ion upper-hybrid frequency where $\omega_{pi} = \sqrt{4\pi n e^2/m_i}$ is the ion plasma frequency], the extraordinary hydromagnetic wave becomes a wave whose natural frequency approaches Ω. More importantly, *Stix* (1958) found that when an IC wave propagates in a plasma along a weakening B, ω becomes enhanced; in the vicinity of $\omega = \Omega$, wave energy can be absorbed by the plasma via cyclotron damping with extremely efficient power transfers. At the same time, *Bernstein* (1958) studied extensively electron and ion oscillations of a fully ionized, collision-free plasma in a static external magnetic field. For the low-frequency ion oscillations, he predicted two modes at cyclotron harmonics: longitudinal ion waves and transverse hydromagnetic waves.

Stix's effective plasma heating mechanism drew much attention in theoretical and laboratory plasma studies. The energization process was soon confirmed by experiments on a magnetic mirror device called the B-66 machine (*Hooke et al.* 1961). Besides, another experiment performed in cesium and potassium plasmas also observed the IC oscillations when the electron drift was $\sim$10 times the ion thermal velocity, but the frequency was slightly higher than Ω (*D'Angelo & Motley* 1962). At the same time, *Drummond*

& *Rosenbluth* (1962) explained that the IC oscillations was excited by the magnetic field-aligned currents (FACs), and *Woods* (1962) extended *Stix*'s work by taking into consideration the effects of the plasma viscosity and compressibility. By using a generalized dispersion relation, the author showed that a range of oscillation frequencies is possible which are well beyond Ω. Furthermore, *Yoshikawa et al.* (1965) showed that the ion heating is also contributed by the electron Landau damping and electron-ion collisions. Later, *Hosea & Sinclair* (1969,1970) exposed that even the IC wave propagation in a plasma is influenced by the electron inertia. In an experiment where torsional Alfven waves were excited, *Müller* (1974) examined the coupling of ions with neutrals with a decreasing ionization degree. He witnessed that both k and the damping effect peaked at Ω.

Interestingly, the IC-resonance acceleration principle was soon applied to separate ion isotopes and ions with different charge-to-mass ratios in plasmas (*Dawson et al.* 1976; *Weibel* 1980). But if a plasma contains only two ion species, Sawley & Tran (1982) noticed that the IC frequency lies approximately midway between the two Ω values. For a plasma including more than one ion species, Sawley (1990) and Sawley & Paris (1990,1991) demonstrated that IC modes are strongly influenced by electron dynamics (the electron inertia and Landau damping) in a low density plasma cavity, just as revealed in the plasma with one type of ions by *Yoshikawa et al.* (1965). Another important result was obtained by *Ono et al.* (1984). The authors measured profiles of wave absorptions versus ion temperatures in an ACT-1 hydrogen plasma. They identified that the excellent efficient IC resonant heating occurs near the fifth IC harmonics of deuterium-like and tritium-like ions. It deserves to mention an intriguing experiment designed by *Sato & Hatakeyama* (1985). The authors used a voltage-biased electrode to drive an IC oscillation. The potential penetrates into a plasma channel parallel to B in front of the electrode, whileas the penetration is limited by the radial escape of ions from the plasma channel. This radial escape was found to obey the cyclotron motion with a period of Ω in the region close to the electrode.

In a plasma containing both negative and positive ions, *D'Angelo & Merlino* (1986) and *Song et al.* (1989) found that there are two branches of the IC modes for $m_{i+} > m_{i-}$: One is the "low-frequency" mode $\omega \geq \Omega_+$, and the other is the "high-frequency" one $\omega \geq \Omega_-$. The frequencies were found to increase with the increasing percentage of negative ions. Particularly, by employing the standard linear Vlasov theory, *Chow & Rosenberg* (1995,1996) investigated the effects of heavier dust and heavier negative ions on the collisionless IC instabilities, respectively. In the former case, the authors showed that positively charged dust tends to stabilize IC waves, while negatively charged dust facilitates triggering the instability; in the latter case, by contrast, the instabilities of both the light and heavy ions are easier to be excited when more charge is carried by negative ions. In both cases, the critical electron drifts to excite the instabilities decrease when the relative density of negative ions increases. In another dusty plasma experiment to observe the IC waves, *Barkan et al.* (1995) verified that negatively charged dust makes the plasma more unstable. The newest experimental work was done by *Kim et al.* (2008). They used very heavy negative ions $(C_7F_{14}^-)$ in the plasma and observed that these ions increase both the number and the intensity of the excited harmonic IC modes.

In geospace, especially in auroral regions, electrostatic IC oscillations have been detected by rockets and satellites. Early space-borne measurements of harmonic IC oscillations in the VLF bands were done by, e.g., *Smith et al* (1964), *Gurnett et al* (1965), *Mosier & Gurnett* (1969), *Kikuchi* (1970) at altitudes <2700 km. Following these measurements, numerous vehicles diagnosed IC oscillations during last decades, such as S3-3 (*Kintner et al.* 1978), DE-1 (*Boardsen et al.* 1990; *Erlandson & Ukhorskiy* 2001), ISEE-1 (*Guglielmi et al.* 2000), Polar (*Mursula et al.* 2001), FAST (*Chaston et al.* 2002), and Cluster (*Backrud* 2005). Because many observations provided evidence of parallel electric fields and/or field-aligned currents existing in regions where IC waves were measured, the excitation of the IC waves was naturally connected to the current-driven mechanism as considered by laboratory experiments and theoretical studies (e.g., *Schunk & Walker* 1970). It was suggested that if the field-aligned currents increase to a threshold, say, tens of $\mu A/m^2$ in strength, the IC instability [and/or the Buneman instability, the ion acoustic (IA) instability] can be triggered; the plasma turbulence and then anomalous collisions thus induced in turn moderate the currents via anomalous transport coefficients (*Kindel & Kennel* 1971; *Papadopoulos* 1977). This process was considered to lead to two possible conspicuous consequences: one is the formation of nonwave phase-space clumps originated from

the growth of the plasma instability (*Chiueh & Diamond* 1986), and the other is the enhanced Joule heating in plasmas due to the anomalous resistivity (*St.-Maurice* 1987).

By excluding any nonlinear dispersion relations, viscous heating terms, and chemical reactions, *Forme et al.* (1993) presented the criteria for the wave ignitions due to current-driven instabilities. The authors brought to light following results by using an isotropic, time-dependent model: (1) If $v_{de} > 1.8v_{the}$ (where v_{de} and v_{the} are electron drift velocity and thermal velocity, respectively), the Bunemann instability is initiated. The heating rates obey $\frac{\partial T_e}{\partial t} = \frac{2}{3}\frac{m_e}{k}v_{de}^2\nu_e^*$ and $\frac{\partial T_i}{\partial t} \sim \frac{m_e}{m_i} \cdot \frac{\partial T_e}{\partial t}$ [where T_e, T_i, m_e, and k are the electron temperature, ion temperature, electron mass, Boltzmann constant, respectively, $\nu_e^* = \alpha\left(\frac{m_e}{m_i}\right)^{1/3}\omega_{pe}$ the electron anomalous collision frequency, α the numerical coefficient, and ω_{pe} the electron plasma frequency]. (2) If $v_{de} > \frac{T_i}{T_e}v_{the}$, the IA instability starts. The heating rates follow $\frac{\partial T_e}{\partial t} = \frac{2}{3}\frac{m_e}{k}v_{de}^2\nu_e^*$ and $\frac{\partial T_i}{\partial t} \sim \frac{\frac{T_e}{T_i}\frac{C_s}{v_{de}}}{1-\frac{C_s}{v_{de}}} \cdot \frac{\partial T_e}{\partial t}$ [in which $\nu_e^* = 10^{-2}\alpha\left(\frac{T_e}{T_i}\right)\left(\frac{v_{de}}{v_{the}}\right)\omega_{pe}$, and $C_s = \sqrt{\frac{m_e}{2m_i}\left(1+\sqrt{1+12\frac{T_i}{T_e}}\right)} \cdot v_{the}$ is the generalized sound velocity]. (3) If $v_{de} > v_e = 15\frac{T_i}{T_e}v_{thi}$, the IC instability begins. The heating rates take $\frac{\partial T_e}{\partial t} = \frac{2}{3}\frac{m_e}{k}v_{de}^2\nu_e^*$ and $\frac{\partial T_i}{\partial t} = \frac{2}{3}\frac{m_i}{k}v_{de}^2\nu_i^*$ [in which $\nu_e^* = \alpha\Omega_i\left(\frac{v_{de}}{v_e}-1\right)^2$, and ν_i^* is the ion anomalous collision frequency satisfying $m_i\nu_i^* = m_e\nu_e^*$]. Numerical calculations exhibited that the first two instabilities produce bigger electron heating rates due to much higher collision frequencies which inhibit the electron heat conduction processes, while the first instability contributes little to the ion temperature ratio, and the IC instability seems to be initiated at the lowest altitudes while all of them should exist above 1000 km for strong currents with tens of μA/m^2.

Obviously, within the scope of linear plasma waves, IC oscillations can be reasonably explained by current-driven mechanism. Nevertheless, as foretold by *Bernstein, Green, & Kruskal* (BGK) (1957) that localized non-wave phase-space structures may exist in turbulent plasmas originated from nonlinear processes, numerous studies have demonstrated that coherent, nonlinear potential structures can actually be triggered by the particle trapping due to various wave-particle interactions (see a review given by *Eliasson & Shukla* 2006). Specifically, there are three stages in the development (*Büchner & Elkina* 2006): (1) Electrons are switched from a free state to a trapped state in a potential well, leading to the formation of electron phase-space holes by instabilities; (2) The potential structures grow and deepen with the growth of electron phase-space holes; the anomalous transport properties increase to develop ion trapping; and (3) After several ion cyclotron periods, localized non-wave structures (also called solitary waves, space-charge elements, electrostatic double layers, clumps, or electrostatic shocks) are formed in phase space. If both waves and non-wave structures remain alive in electric and magnetic fields, the space-charge structures are stratified (or "filamented") to form field-aligned "clumps" (*Dupree* 1972); at the same time, ions response to these elements in two possible ways: they may either keep regular motions without any gains of the electromagnetic energy from the fields if their speed across the magnetic field is less than the phase velocity of a single wave (*Karney & Bers* 1977), or, be coherently energized within a small phase space when the Doppler-shifted wave frequencies are close to an integer multiple of Ω (*Strozzi et al.* 2003).

In the IC modes, *Chiueh & Diamond* (1986) discovered that if $T_{\perp i} \geq T_{\parallel i} \sim T_e$ (where $T_{\perp i}$ and $T_{\parallel i}$ are ion temperature components perpendicular and parallel to B, respectively), the turbulence is of the wave-clump type; if $T_{\perp i} \gg T_{\parallel i} \sim T_e$, it is the clump-dominant type. This new ingredient is space-charge "clumps", the so-called electrostatic solitons, which describes the incomplete blending of a Vlasov plasma: wave-particle interactions make stochastic orbits of particles by turbulent electric fields; the phase-space density tends to decrease to smaller scales in a finite time, and thus generate phase-space space-charge density granulations (that is, clumps); these clumps ballistically propagate at the resonant velocities $v = \omega - n\Omega_i/k_{\parallel}$ in a finite time. In the development, the turbulent forces produced by the turbulent electromagnetic field tend to tear the space-charge chunk of particles apart and cause the decay of the clumps. However, the size of the space-charge structures is so small that they keep every particle feels the same force. Thus, the elements retain their structural integrity for a relatively longer time than the average correlation time of the system. This effect offsets the separation tendency caused by turbulent processes.

In addition, the authors found that the shape of the space-charge structures does not rely on turbulent frequencies in position space, but does in velocity space. In position space, for either low or high frequency turbulence, the parallel scale is of the spectrum-averaged parallel wavelength $\bar{k}_\parallel^{-1}$, while the perpendicular scale is of the cylindrically-symmetric, spectrum-averaged perpendicular wavelength $\bar{k}_\perp^{-1}$. By contrast, in velocity space, the perpendicular extent is not the same for different frequency bands: for low-frequencies, the scale can extend up to a scale dependent on the thermal velocity v_T; for high frequencies, it is determined by $v_T(\bar{k}_\perp \rho)^{-1} > v_T$ (where $\rho = \frac{v_T}{\sqrt{2}\Omega}$ is the gyroradius, and $\bar{k}_\perp \rho \geq 1$). Specifically, the clump shape in phase space depends on the particle species. For electron clumps in the IC regime, the perpendicular diffusion dominates the parallel one with $\bar{k}_\perp \gg \bar{k}_\parallel$. So electron parallel diffusion can be ignored. Because electrons are strongly magnetized with $\bar{k}_\perp \rho_e \ll 1$, electron clump is bounded to the magnetic field lines. In real space, it has a 1-D long cigar shape. In velocity space, it has a pancake shape of radius v_{te} and thickness $(\bar{k}_\parallel \tau_e)^{-1}$ (where τ_e is the electron decorrelation time). The electron clump travels at a parallel speed of $v_\parallel \sim n\Omega_i/k_\parallel$. For ion clumps, their perpendicular diffusion is dominated by $\bar{k}_\perp \gg \bar{k}_\parallel$, like electron ones. So ion parallel diffusion can also be ignored. However, ions are weakly magnetized with $\bar{k}_\perp \rho_i \sim 1$. If $\bar{k}_\perp \rho_i < 1$, ion clump will show the same cigar shape as electron clump in real space. On the other hand, if $\bar{k}_\perp \rho_i > 1$, ion clump will appear as a tether rod in real space with tether length ρ_i gyrating about the guiding center (GC). In both cases, the ion clump propagates at the ballistic velocity v with a radius $\bar{k}_\perp^{-1}$ and a length $\bar{k}_\parallel^{-1}$. In velocity space, ion clump appears in a pancake shape of radius v_{ti} for $\bar{k}_\perp \rho_i < 1$, and in a gyrating tether disk of radius $v_{ti}(\bar{k}_\perp \rho_i)^{-1}$ and tether length v_{ti} for $\bar{k}_\perp \rho_i > 1$. The thickness of either the pancake or the disk is $(\bar{k}_\parallel \tau_i)^{-1}$ (where τ_i is the ion decorrelation time).

The nonlinear space-charge structures have been observed at many sites in geospace, e.g., auroral zones of mid-and-high-altitudes, bow shock, magnetotail, and solar wind due to the existence of detectable space-charge electric fields, see, e.g., *Mottez* (2001) for detailed introductions. The nonlinear phenomena had been recognized gradually with the advance of theoretical work and observations (*Pickett et al.* 2005). The structures were first noticed and named as intense broadband electrostatic noises (BENs) in 1970s in the magnetotail (*Scarf et al.* 1974; *Gurnett et al.* 1976), along with data of magnetic noise bursts (relating to cross-tail current and intervals of tailward flows), electrostatic electron cyclotron waves, and upper hybrid waves (*Gurnett et al.* 1976; *Cattell et al.* 1986). BEN is bursty, extending from the lowest frequencies up to as high as the plasma frequency (electron cyclotron frequency) while the intensity decreases when the frequency increases. It peaks at or below the LH frequency. During 1980s, the first space-charge structure was identified from S3-3 waveform electric-field data in the auroral acceleration region (*Temerin et al.* 1982). It is characterized by locally density-depleted (called "ion hole"), electric-field fluctuations in a size of Debye-scale. Because no spectral form of data were used, no link was made between these new definitions and BEN, but simply the FFT-rendering of solitary waves. Yet, theoretical investigations pointed out that certain kinds of nonlinear structures could explain the broad frequency spectra (*Nishida et al.* 1985), and, electron acoustic solitons passing by a satellite would generate spectra that could explain the high frequency part of BEN (*Dubouloz et al.* 1991). The breakthrough eventually came when a sophisticated waveform receivers was used, which has a high temporal resolution. In 1994, *Matsumoto et al.* (1994) analyzed the distant magnetotail with Geotail data and proved that solitary waves are as a matter of fact BENs: the measured waveform electric field of BENs is nothing but the spectra from of the electrostatic solitary waves carrying space-charge electric fields. From that time, extensive and detailed pictures for these nonlinear electric field structures were reported from almost every high-resolution space project (see details in *Ma & Hirose* 2009), e.g., S3-3 (*Temerin et al.* 1982), Viking (*Boström et al.* 1988), Geotail (*Matsumoto et al.* 1994), Wind (*Bale et al.* 1998), FAST (*Ergun et al.* 1998a,b,c; *McFadden et al.* 1999; *McFadden et al.* 2003), Polar (*Mozer et al.* 1997; *Franz et al.* 1998; *Bounds et al.* 1999; *Cattell et al.* 1999; *Franz et al.* 2000), and Cluster (*Pickett et al.* 2004; *Pickett et al.* 2005). What is more, these structures explain FAST-measured transverse ion heating in auroral magnetosphere (*Ma et al.* 2009).

It is now clear that the electrostatic solitary waves are solitary structures that behave as are space-charge carriers to contribute strong transverse electric fields to space plasmas. Due to the presence of these fields, the characteristics of charged particles residing in the vicinity of the regions teemed with

solitary waves will surely be altered. For example, in his pioneer work, *Stix* (1957) showed unequivocally that near the IC resonant frequency the electric field determines the behavior of charged particles. This prediction was demonstrated to be valid by *Cole* (1976). He showed that the virtual ion cyclotron frequency ω should satisfy $\omega^2 = \Omega^2 + \Omega d(E_x/B)/dx$ when the first derivative of the electric field $(\nabla \cdot \mathbf{E} = dE_x/dx)$ is nonzero, while the second derivative (d^2E_x/dx^2) is zero. Another example was given by *St.-Maurice et al.* (1994). If $\mathbf{E} = E_0(1 + y/L)\hat{\mathbf{y}}$ in the cartesian geometry (where E_0 is the field at $y = 0$, L the characteristic length, y the ion position), that is, the electric field is proportional to the distance in a specific direction in space, the authors exposed that $\omega^2 = \Omega^2[1 - (E_0/B)/(L\Omega)]$. In the cylindrical case, *Ma & St.-Maurice* (2008) also presented that $\omega^2 = \Omega^2[1 + 4(E_c/B)/(R_c\Omega)]$ if $\mathbf{E} = -E_c(r/R_c)\hat{\mathbf{r}}$ (where E_c is the field at $r = R_c$, R_c the characteristic radius, r the ion position), that is, the electric field is proportional to the radius. These studies unfolded that the frequency of the IC oscillations can shift away from Ω either positively or negatively, depending on the polarization of E perpendicular to B, but irrelevant of the origin of E. In the linear wave regime, the perturbed E is weak. The frequency shift is thus negligible. On the contrary, if E is provided by some nonlinear process, say, the space charges of solitons, the linear perturbation condition is broken. E may be so strong that the shift is unable to be overlooked. Let's use FAST data for an estimation. *Ergun et al.* (1998c) provided that the local magnetic field B is 11481 nT, and the typical peak strength of the space-charge electric field E for a soliton is 1 V/m. As a result, the local peak $\mathbf{E} \times \mathbf{B}$ drift (E/B) is 87 km/s. At the thermal equilibrium state of about 1000 K, the thermal speeds of protons and electrons are of the orders of 4 km/s and 170 km/s, respectively. The speed E/B is typically larger than the ion thermal speed. However, the speed E/B is small relative to the electron thermal speed. Any departures from a Maxwellian velocity distribution due to the Lorentz force cannot be negligible for ions, and we call such a electric field is "strong" for ions. In such strong fields, any traditional linear wave theory is not suitable to be used. But for thermal electrons, they can still be simply assumed to follow Maxwellian but with a $\mathbf{E} \times \mathbf{B}$ drift to the leading order for the situation at hand. We call such a electric field is "weak" for electrons, and traditional linear wave theories are still valid for them.

Let's use FAST data to assess the cyclotron frequency ω of ions in the strong electric field mentioned above, in order to know the order of the frequency shift. Assume that the field is cylindrically symmetric and proportional to r. The magnetic gyrofrequency of ions is $\Omega_i = 1100$ rad/s (or 200 Hz) for a proton, and $\Omega_e = (m_i/m_e)\Omega_i$ for an electron. R_c scales with the ion gyroradius ρ_i which satisfies $2\lambda_D \leq \rho_i \leq 20\lambda_D$ where $\lambda_D = 82$ m is Debye length (*Ergun* 1999). These parameters give $1.1\Omega_i \leq \omega \leq 1.7\Omega_i$, indicating that the IC oscillation ω always deviates from Ω_i by tens of percent. For a plasma density of $n_0 \sim 5.7$ cm^{-3}, we have the ion plasma frequency ω_{pi} is 3139 rad/s, and the electron plasma frequency ω_{pe} is $43\omega_{pi}$. Thus, the lower-hybrid (LH) frequency ω_{LH} is 3138 rad/s (or 500 Hz). Obviously, the maximum IC oscillation frequency shifts into the LH band. This approximate evaluation explains qualitatively the FAST observations that the solitary structures are evenly spaced at a frequency above the local H^+ gyrofrequency (see Fig.5 in *Ergun et al.* 1998c for a reference). Notice that this estimation is only suitable for a single soliton case. In reality, the electric field should be produced by space charges of all soliton trains in magnetic flux tubes; and, the strength of E may not be constant with time. Therefore, the IC oscillations may have a very different picture. More detailed modeling and simulations are then needed for accurate data assimilations and quantitative explanations. Unfortunately, no relevant studies have been found to report on the IC oscillations under strong electric field conditions. This situation is understandable: traditionally, we rely on the linear plasma wave theory to consider instabilities and related oscillations, where the wavefield E is weak, behaving as a perturbation, and that measured ω should always be located at harmonics of Ω; any observable deviations from linear theory predictions are naturally attributed to the contributions of unusual initial and/or boundary conditions within the frame of the theory, regardless of the fact whether or not these conditions are still valid for the theory.

Fortunately, stochastic methods are widely used in different fields of physics, as given in references of, e.g., *Bonfig* (1988); *Vojko et al.* (1994); *Vojko & Dali* (1996). Different these methods, we offer an alternative approach in this paper which illustrates the IC oscillations stimulated by a strong electric field of solitons propagating in auroral ionosphere. The electric field is produced by solitons' space charges stochastically in the plane perpendicular to the magnetic field. We focus on the ion oscillating
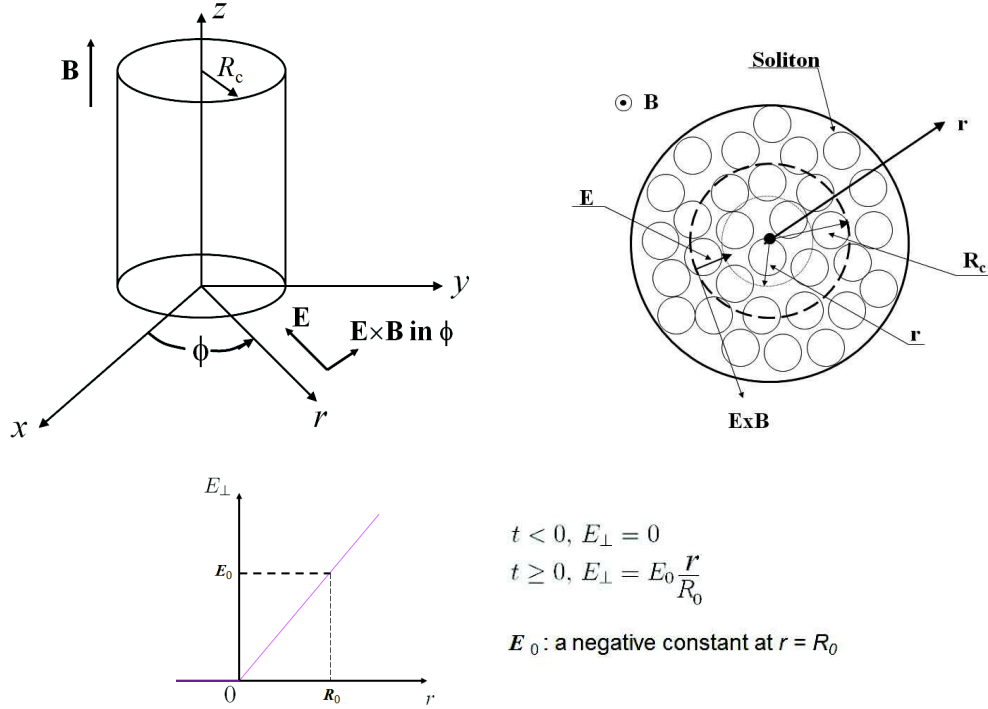
$$t < 0, \ E_\perp = 0$$
$$t \geq 0, \ E_\perp = E_0 \frac{r}{R_0}$$

E_0: a negative constant at $r = R_0$

Fig. 1 Left: Cylindrical coordinates with reference to the Cartesian frame of an infinitely-long magnetic flux tube, the symmetric line of which lies on the z-axis. R_c is a characteristic radius. Right: A cross-section viewed from the top. The flux tube is teeming with a dense cluster of soliton trains (*Ergun et al.* 1998c; *Ergun* 1999). The diagram is not to true scale, but used to dramatically illustrate the point. Adapted from *Ma et al.* (2009).

feature, in order to see what kind of frequency-shifted IC waves can be excited. This study is totally different from those using traditional linear wave theories where the plane-wave perturbation assumption, $\mathbf{E}_1 \sim e^{i(\mathbf{k}\cdot\mathbf{r}-\omega t)}$, is used. For strong space-charge electric field strengths which produce large drifts to particles, this weak-field condition is broken and we have to seek for solutions with the aid of kinetic theory, and then to describe the macroscopic properties of ions in terms of their microscopic characteristics of motion. We start from setting up a physical model to describe solitons propagating in a magnetic flux tube, and give a Hamiltonian formulation for ions driven by the space-charge electric field in the tube, as given in Section 2. Then, in Section 3, we present results for the IC oscillation features and bulk parameters of ions with a nonzero initial drift velocity by solving directly the Boltzmann equation coupled with ion equations of motion in a temporally-constant electric field (note that this "constant" occurs only instantaneously for a stochastic field). To give a clear illustration for the IC oscillations in solitons' stochastic electric field, we relax the "constant" condition in Section 4 by using an artificial stochastic $\mathbf{E}$ which has 10-step random strengths in corresponding 10 different time intervals. The accommodation of ω (as well as other parameters) is illustrated in response to the $\mathbf{E}$ switches. At last, the work is generalized by using two random-number generators for the strength and time, respectively, in Section 5. In Section 6, we summarize the results and have a discussion. The last Section gives conclusions.

2   Physical modeling of nonlinear waves

In order to provide the most basic picture for the new mechanism, and thus to gain important insights into more complicated situations, while still being able to illustrate the process clearly, we set up a physical model in a cylindrical geometry (r, ϕ, z) for a dense cluster of soliton trains propagating in a magnetic flux tube with the axis along the magnetic field $\mathbf{B} = B\hat{\mathbf{e}}_z$ (where $\hat{\mathbf{e}}_z$ is the unit axial vector), which is assumed to be homogeneous in space, as described by Fig.1. The background to set up such a model is identical to what was presented in *Ma* & *St-Maurice* (2008) where we focused on the auroral region which is in and above 140 km, well with the F-layer. In this region, numerous data were collected by satellites, radars and rockets which exposed the existence of solitary waves, as introduced in the above Section. Based on previous studies, this region owns a magnetic field of 0.5 Gauss; ion temperature of 1000 K; stochastic transverse electric fields up to an order of 50 mV/m or greater; an ion-neutral collision frequency of an order of 0.01-1 Hz; and, ion gyrofrequency of an order of 50 Hz. See *Ma* & *St-Maurice* (2008, 2015) in details. The consideration of the modelling is inspired by FAST observations (see, e.g., *Ergun et al.* 1998c; *Ergun* 1999) which provided the features of the soliton cluster in the tube as follows (*Ma et al.* 2009):

(1) the cluster is composed of infinite long cylindrically-symmetric trains of solitons;

(2) each of the trains appearing in space has the same space-charge density δn_{sc};

(3) both the number and time are random for trains to emerge in space due to the plasma turbulence;

(4) space charges carried by all the trains arising in space cause a homogeneous density perturbation to the uniform and isotropic background n_0;

(5) the cylinder-edge effects are neglected with a characteristic radius R_c of a circle (heavy dashed line) which is well inside the flux-tube cylinder (heavy solid boundary line);

(6) the electron-electron, electron-ion, electron-neutral, and, ion-neutral interactions are neglected, and thus we are dealing with a collision-free problem.

Under these simplifications, the space-charge density of the whole cylinder, δn_c, should be δn_{sc} if the flux tube is completely filled with soliton sets. However, soliton trains appear in space stochastically. Thus, δn_c is stochastic, denoted by $\delta \tilde{n}_c$, where and hereafter the sign " ˜ " means "stochastic". This stochasticity originates from the probabilistic magnitude and appearance of δn_c in the flux tube. In the area within the radius r (thin solid line), $\delta \tilde{n}_c$ produces a radial electric field $\tilde{E}_r$ by means of Gauss's law if we assume that solitons have electron space charges:

$$\tilde{E}_r = -\tilde{E}_c r \tag{1}$$

where $\tilde{E}_c = [eR_c/(2\epsilon_0)]\delta\tilde{n}_c$ is positive. Clearly, the electric field within the cylinder is proportional to r, and points radially inward. We can check that the plasma is quasi-neutral even if the plasma has a density perturbation: if we were to let $\tilde{E}_c$=2 V/m at R_c=1 km, the corresponding space-charge number density would need to be $\delta\tilde{n}_c \approx 2 \times 10^5$ m^{-3}. This is 10^4 to 10^6 times smaller than the ambient plasma density n_0 in the ionospheric F-region. In such a radial electric field proportional to r, at any time before $\tilde{E}_c$ switches to a new amplitude next, ion dynamics are determined by the electrostatic, space-charge electric field (crossed to $\mathbf{B}$) which is constant with time at the present step. We study the ion oscillations starting from $t = 0$ when the electric field $\tilde{E}_r$ is applied, and ions have an initial state with a Maxwellian distribution function, but the initial guiding-center (GC) velocity $\mathbf{v}_{d0}$ of ions (or, the drift velocity exhibiting the initial state of the ion's instantaneous center in velocity space) is nonzero.

We are going to deal with a system of a nonrelativistic ensemble of ions of the same species in the absolute space. The particles are assumed identical, and a test particle thus provides an idealized approximation to exhibit physical properties of the specified domain (*Gartenhaus* 1964; *Schmidt* 1979; *Humphries* 1990). We use the ion's Hamiltonian formulism as the radical basis for the study:

$$H = \mathbf{p} \cdot \mathbf{v} - L \ , \quad L = \mathcal{K} - P \tag{2}$$

in which H is the Hamiltonian, $\mathbf{p} = \{p_r, p_\phi, p_z\}$ is the canonical momentum, $\mathbf{v} = \{v_r, v_\phi, v_z\} = \{\dot{r}, r\dot{\phi}, \dot{z}\}$ is the velocity, L is the Lagrangian, $\mathcal{K} = \frac{1}{2}m_i\mathbf{v}^2$ is the kinetic energy, $P = e(\varphi - \mathbf{v} \cdot \mathbf{A})$ is the potential

energy, where $\varphi(r) = -\int \mathbf{E} \cdot \mathrm{d}\mathbf{r} = \frac{1}{2}\tilde{E}_c R_c \cdot (r/R_c)^2$ is the electric potential, and $\mathbf{A}$ is the vector potential satisfying $\mathbf{B} = \nabla \times \mathbf{A}$. In cylindrical coordinates,

$$\mathcal{K} = \frac{1}{2}m_i(\dot{r}^2 + r^2\dot{\phi}^2 + \dot{z}^2) \ , \quad P = e\left[\frac{1}{2}E_c R_c \left(\frac{r}{R_c}\right)^2 - \frac{1}{2}Br^2\dot{\phi}\right] \tag{3}$$

where and hereafter $\tilde{E}_c$ is written as E_c for simplicity. These two expressions give

$$\tag{4}$$

$$\left.\begin{array}{l} L = \frac{1}{2}m_i(\dot{r}^2 + r^2\dot{\phi}^2 + \dot{z}^2) - e\left[\frac{1}{2}E_c R_c \left(\frac{r}{R_c}\right)^2 - \frac{1}{2}Br^2\dot{\phi}\right] \\ p_r = \partial L/\partial\dot{r} = m_i\dot{r} \\ p_\phi = \partial L/\partial\dot{\phi} = m_i r^2\dot{\phi} + \frac{1}{2}eBr^2 \\ p_z = \partial L/\partial\dot{z} = m_i\dot{z} \end{array}\right\} \tag{5}$$

and then,

$$H = \frac{1}{2}m_i v_r^2 + \frac{1}{2}m_i v_\phi^2 + \frac{1}{2}m_i v_z^2 + \frac{1}{2}m_i\frac{E_c}{B}R_c\Omega\left(\frac{r}{R_c}\right)^2 \tag{6}$$

in which $\Omega = eB/m_i$ is the ion gyrofrequency. Using the two canonical Hamilton's equations of motion, $\dot{\mathbf{r}} = \partial H/\partial\mathbf{p}$ and $\dot{\mathbf{p}} = -\partial H/\partial\mathbf{r}$, we obtain:

$$\ddot{r} = r(\dot{\phi}^2 + \Omega\dot{\phi}) - \frac{E_c}{B}R_c\Omega\frac{r}{R_c^2} \ , \quad r\ddot{\phi} = -2\dot{r}\dot{\phi} - \Omega\dot{r} \ , \quad \ddot{z} = 0 \tag{7}$$

Because the time-inversion transformation has an unaltered nature (*Gartenhaus* 1964), that is, for the inversion of the time direction ($t \to -t$), there exist ($\mathbf{r} \to \mathbf{r}$) and ($\mathbf{v} \to -\mathbf{v}$), we know that the position vector $\mathbf{r}$ and hence all quantities that depend only on $\mathbf{r}$ do not change sign; by contrast, the velocity vector $\mathbf{v}$ and quantities that depend only on $\mathbf{v}$ change sign. This property gives that for two states $\{\mathbf{r}_1, \mathbf{v}_1, t_1\}$ and $\{\mathbf{r}_2, \mathbf{v}_2, t_2\}$ of a particle, there are two identical solutions for the same equation of motion. One provides expressions of $\{\mathbf{r}_1, \mathbf{v}_1, t_1\}$ by using $\{\mathbf{r}_2, \mathbf{v}_2, t_2\}$, and the other is to express $\{\mathbf{r}_2, \mathbf{v}_2, t_2\}$ by $\{\mathbf{r}_1, \mathbf{v}_1, t_1\}$, whereas the description of the characteristics of motion is unaltered. That is to say, we can either use the initial state as the final state, or, vice versa. For ions, Eq.(6) provides three constants of motion due to the fact that the Hamiltonian does not contain ϕ, z, and time t explicitly: the azimuthal angular momentum $p_\phi = K$, the axial momentum p_z, and the total energy H. Expressed by the parameters at the two states, we have

$$\left.\begin{array}{l} p_\phi = m_i r_1 v_{\phi 1} + m_i r_1^2\frac{\Omega}{2} = m_i r_2 v_{\phi 2} + m_i r_2^2\frac{\Omega}{2} = K \\ p_z = m_i v_{z1} = m_i v_{z2} \\ H = \frac{1}{2}m_i v_{r1}^2 + \frac{1}{2}m_i v_{\phi 1}^2 + \frac{1}{2}m_i v_{z1}^2 + \frac{1}{2}m_i\frac{E_c}{B}R_c\Omega\left(\frac{r_1}{R_c}\right)^2 = \\ \qquad = \frac{1}{2}m_i v_{r2}^2 + \frac{1}{2}m_i v_{\phi 2}^2 + \frac{1}{2}m_i v_{z2}^2 + \frac{1}{2}m_i\frac{E_c}{B}R_c\Omega\left(\frac{r_2}{R_c}\right)^2 \end{array}\right\} \tag{8}$$

in which $\{r_1, v_{r1}, v_{\phi 1}, v_{z1}\}$ and $\{r_2, v_{r2}, v_{\phi 2}, v_{z2}\}$ the parameters of $\{r, v_r, v_\phi, v_z\}$ at $t = t_1$ and $t = t_2$, respectively. Thus, in the plane perpendicular to $\mathbf{B}$, we obtain two Hamilton's canonical equations:

$$\left.\begin{array}{l} r_1 v_{\phi 1} + r_1^2\frac{\Omega}{2} = r_2 v_{\phi 2} + r_2^2\frac{\Omega}{2} = K/m_i \\ v_{r1}^2 + v_{\phi 1}^2 + \frac{E_c}{B}R_c\Omega\left[\left(\frac{r_1}{R_c}\right)^2 - \left(\frac{r_2}{R_c}\right)^2\right] = v_{r2}^2 + v_{\phi 2}^2 \end{array}\right\} \tag{9}$$

corresponding to the conservation of canonical angular momentum and that of the total energy, respectively. Concisely, Eq.(9) gives one modified Hamilton's canonical equation of motion:

$$\left.\begin{array}{l} v_{r1}^2 + \left(\frac{\Omega r_1}{2}\right)^2 + \left(\frac{K}{m_i r_1}\right)^2 + \frac{E_c}{B}R_c\Omega \cdot \left[\left(\frac{r_1}{R_c}\right)^2 - \left(\frac{r_2}{R_c}\right)^2\right] = \\ = v_{r2}^2 + \left(\frac{\Omega r_2}{2}\right)^2 + \left(\frac{K}{m_i r_2}\right)^2 \end{array}\right\} \tag{10}$$

3   Ion cyclotron frequency ω when $\tilde{E}_r$ switches on at $t = 0$

Let moment $t_1 = t$ be the final stage with phase space parameters $\{r, v_r, v_\phi, t\} = \{r_1, v_{r1}, v_{\phi 1}, t_1\}$, and moment $t_2 = t_0 = 0$ be the initial stage with $\{r_0, v_{r0}, v_{\phi 0}, 0\} = \{r_2, v_{r2}, v_{\phi 2}, t_2\}$ (hereafter we will use the subscript '0' to indicate the initial state). Eq.(10) becomes

$$\left.\begin{aligned} v_r^2 + \left(\tfrac{\Omega r}{2}\right)^2 + \left(\tfrac{K}{m_i r}\right)^2 + \tfrac{E_c}{B} R_c \Omega \cdot \left[\left(\tfrac{r}{R_c}\right)^2 - \left(\tfrac{r_0}{R_c}\right)^2\right] = \\ = v_{r0}^2 + \left(\tfrac{\Omega r_0}{2}\right)^2 + \left(\tfrac{K}{m_i r_0}\right)^2 \end{aligned}\right\} \tag{11}$$

Following exactly the same algebra as given in *Ma & St-Maurice* (2008), we obtain the solution of Eq.(11) in the case when the initial GC velocity $\mathbf{v}_d$ is nonzero, namely, $\mathbf{v}_{d0} = \{v_{dr0}, v_{d\phi 0}\} \neq \mathbf{0}$:

$$\left.\begin{aligned} a_0 \left[(v_r - v_{dr})^2 + (v_\phi - v_{d\phi})^2\right] &= a_{00} \left[(v_{r0} - v_{dr0})^2 + (v_{\phi 0} - v_{d\phi 0})^2\right] \\ v_{dr}^2 + \left(v_{d\phi} - \tfrac{E_c}{B}\tfrac{r}{R_c}\right)^2 &= v_{dr0}^2 + \left(v_{d\phi 0} - \tfrac{E_c}{B}\tfrac{r}{R_c}\right)^2 = R_{\mathbf{v}}^2 \\ a_0 = a_{00}\left\{1 - \tfrac{1}{2}\left[1 - \left(\tfrac{\Omega_i}{\omega}\right)^2\right](1 - \cos\omega t)\right\} &= a_{00}\tfrac{a_1 + a_2\cos\omega t}{a_1 + a_2} \\ a_1 = 1 + a_2 \ , \quad a_2 = 2\tfrac{E_c/B}{R_c \Omega_i} \\ v_{dr} = v_{dr0} - \tfrac{E_c}{B}\tfrac{r}{R_c}\tfrac{a_{00}}{a_0}\tfrac{\Omega_i}{\omega}\sin\omega t \\ v_{d\phi} = v_{d\phi 0} + \tfrac{E_c}{B}\tfrac{r}{R_c}\tfrac{a_{00}}{a_0}\left(\tfrac{\Omega_i}{\omega}\right)^2(1 - \cos\omega t) \end{aligned}\right\} \tag{12}$$

in which $a_{00} = a_0|_{t=0} = 1$ is the initial value of a_0; $R_{\mathbf{v}}$ is the distance between the GC velocity $\mathbf{v}_d$ and the $\mathbf{E} \times \mathbf{B}$ drift velocity $\mathbf{v}_E = \mathbf{E} \times \mathbf{B}/B^2$; ω is the ion cyclotron frequency to be determined later. It is clear that the parameters a_0, v_{dr}, and $v_{d\phi}$ are functions of t and r but irrelevant to velocity components v_r and v_ϕ. In concise vector form, the top two expressions in Eq.(12) are expressed as follows:

$$\left.\begin{aligned} a_0(\mathbf{v} - \mathbf{v}_d)^2 &= a_{00}(\mathbf{v}_0 - \mathbf{v}_{d0})^2 \\ (\mathbf{v}_d - \mathbf{v}_E)^2 &= (\mathbf{v}_{d0} - \mathbf{v}_E)^2 = R_{\mathbf{v}}^2 \end{aligned}\right\} \tag{13}$$

which shows that the motion of ions contains two circular trajectories in velocity space: one is that $\mathbf{v}$ rotates around the GC velocity, $\mathbf{v}_d$, and the other is that GC velocity rotates around the $\mathbf{E} \times \mathbf{B}$-drift velocity. If assuming $\mathbf{v}_{d0} = \mathbf{0}$ in Eqs.(12,13), we immediately obtain results given by Eqs.(16$\sim$20) of *Ma & St-Maurice* (2008), which studied the $\mathbf{v}_{d0} = \mathbf{0}$ case. Fig.3 in that paper showed the two orbits in velocity space with an origin O. As a generalization of that case for $\mathbf{v}_{d0} \neq \mathbf{0}$, the two velocity-vector circles are now in a new frame which has a shifted origin O', as presented in Fig.2. In the new frame, the GC $\mathbf{v}_d$-circle passes through O'.

In the old frame, the initial drift velocity at $t = 0$ is $\mathbf{v}_{d0} \neq \mathbf{0}$, and the $\mathbf{E} \times \mathbf{B}$ drift is still as before: $\mathbf{v}_E = \tfrac{E_c}{B}\tfrac{r}{R_c}\hat{\phi} = \{0, \tfrac{E_c}{B}\tfrac{r}{R_c}\}$. The radius of the $\mathbf{v}_d$-circle is

$$R_{\mathbf{v}} = |\mathbf{v}_{d0} - \mathbf{v}_E| = \sqrt{v_{dr0}^2 + \left(v_{d\phi 0} - \frac{E_c}{B}\frac{r}{R_c}\right)^2} \tag{14}$$

which does not equal to the magnitude $(E_c/B)(r/R_c)$ of the vector $\mathbf{v}_E$. Thus, the origin O is either inside the $\mathbf{v}_d$ circle, or outside it. Fig.2 shows the latter case based on the assumed initial condition: $|\mathbf{v}_{d0} - \mathbf{v}_E| < |\mathbf{v}_E|$.

By contrast, in the new frame, we introduce a "pseudo-electric field": $\mathbf{E}' = -E_c'\tfrac{r}{R_c}\hat{\mathbf{r}}$, satisfying

$$R_{\mathbf{v}} = |\mathbf{v}_E'| = \left|\frac{\mathbf{E}' \times \mathbf{B}}{B^2}\right| = \left|\frac{E_c'}{B}\frac{r}{R_c}\hat{\phi}\right| = \frac{E_c'}{B}\frac{r}{R_c} \tag{15}$$

Thus, Eqs.(14,15) provide

$$\frac{E_c'}{B}\frac{r}{R_c} = \sqrt{v_{dr0}^2 + \left(v_{d\phi 0} - \frac{E_c}{B}\frac{r}{R_c}\right)^2} \tag{16}$$
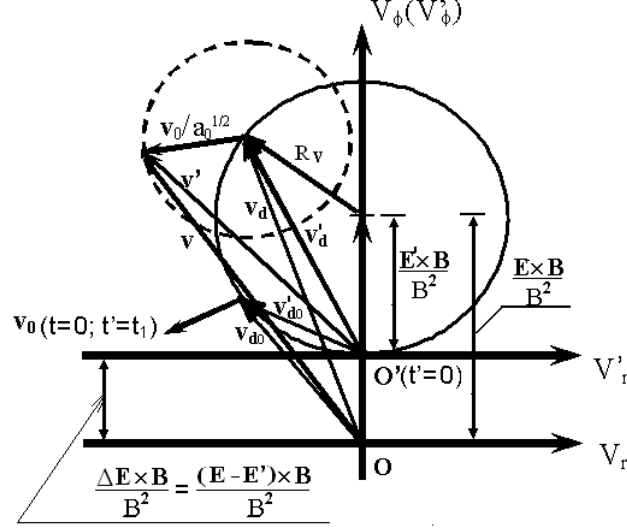
Fig. 2 Characteristics of ion motion for $\mathbf{v}_d$-circle not passing through the origin O. A shifted frame is introduced to satisfy $\mathbf{v}_d$-circle passing through the new origin O'. The relation of the two frames is $v_r = v_r'$ and $v_\phi = v_\phi' + \left|\frac{\Delta\mathbf{E}\times\mathbf{B}}{B^2}\right|$. In the old frame, the initial time is $t = 0$ with $\mathbf{v}_{d0} = \{v_{dr0}, v_{d\phi0}\}$, while in the new one the initial time is $t' = t_1$ with $\mathbf{v}_{d0}' = \{v_{dr0}', v_{d\phi0}'\}$. The initial ion velocity vector $\mathbf{v}_0(t = 0, t' = t_1)$ is also shown, starting from the end of vector $\mathbf{v}_{d0}$ or $\mathbf{v}_{d0}'$.

and then, the difference between $\mathbf{v}_E$ and $\mathbf{v}_E'$ is in the ϕ-direction:

$$\frac{\Delta\mathbf{E}\times\mathbf{B}}{B^2} = \frac{(\mathbf{E}-\mathbf{E}')\times\mathbf{B}}{B^2} = \left\{0, \frac{E_c - E_c'}{B}\frac{r}{R_c}\right\} = \{0, \delta v_\phi\} \tag{17}$$

in which

$$\left.\begin{array}{rcl} \delta v_\phi &=& \frac{E_c}{B}\frac{r}{R_c} - R_\mathbf{v} = \frac{E_c}{B}\frac{r}{R_c}\left(1 - \frac{E_c'}{E_c}\right) = \\[2mm] &=& \frac{E_c}{B}\frac{r}{R_c}\left[1 - \sqrt{\left(\frac{v_{dr0}}{\frac{E_c}{B}\frac{r}{R_c}}\right)^2 + \left(\frac{v_{d\phi0}}{\frac{E_c}{B}\frac{r}{R_c}} - 1\right)^2}\right] \end{array}\right\} \tag{18}$$

Using this shift, we obtain a relation between the old and new frames:

$$v_r' = v_r \ , \quad v_\phi' = v_\phi - \delta v_\phi \tag{19}$$

and the expression of $R_\mathbf{v}$ changes from the old frame to the new one:

$$R_\mathbf{v} = |\mathbf{v}_{d0} - \mathbf{v}_E| = |\mathbf{v}_{d0}' - \mathbf{v}_E'| \tag{20}$$

in which $\mathbf{v}_{d0}' = \{v_{dr0}', v_{d\phi0}'\}$ is in fact the vector $\mathbf{v}_{d0}$ but viewed in the new frame, satisfing

$$(\mathbf{v}_{d0}' - \mathbf{v}_E')^2 = \left(\frac{E_c'}{B}\frac{r}{R_c}\right)^2 \tag{21}$$

Because

$$(\mathbf{v}_d' - \mathbf{v}_E')^2 = (\mathbf{v}_{d0}' - \mathbf{v}_E')^2 \tag{22}$$

in the circular motion at any time $t \geq 0$, we have

$$(\mathbf{v}'_d - \mathbf{v}'_E)^2 = \left(\frac{E'_c}{B} \frac{r}{R_c} \right)^2 \tag{23}$$

in the new frame, or, using the scalar expression,

$$v'^2_{dr} + \left(v'_{d\phi} - \frac{E'_c}{B} \frac{r}{R_c} \right)^2 = \left(\frac{E'_c}{B} \frac{r}{R_c} \right)^2 \tag{24}$$

which indicates that the GC velocity $\mathbf{v}'_d$ passes through the origin O', and there is an initial GC velocity $\mathbf{v}'_{d0} = 0$ at $t' = 0$. Therefore, we have following important relations in the new frame, just as those relations in the case of $\mathbf{v}_{d0} = 0$ at $t = 0$ in the old frame given in *Ma & St-Maurice* (2008):

$$\left. \begin{aligned} a'_0(t') &= a'_{00} \left\{ 1 - \tfrac{1}{2} \left[1 - \left(\tfrac{\Omega}{\omega} \right)^2 \right] (1 - \cos \omega t') \right\} \\ v'_{dr}(t') &= -\frac{E'_c}{B} \frac{r}{R_c} \frac{a'_{00}}{a'_0} \frac{\Omega}{\omega} \sin \omega t' \\ v'_{d\phi}(t') &= \frac{E'_c}{B} \frac{r}{R_c} \frac{a'_{00}}{a'_0} \left(\frac{\Omega}{\omega} \right)^2 (1 - \cos \omega t') \end{aligned} \right\} \tag{25}$$

where

$$\omega = \Omega \sqrt{1 + 4 \frac{E'_c / B}{R_c \Omega}} = \Omega \sqrt{1 + \left(4 \frac{R_c}{r} \right) \frac{R_{\mathbf{v}}}{R_c \Omega}} \tag{26}$$

in which Eq.(16) is used. This expression gives the IC frequency in the case of $\mathbf{v}_{d0} \neq 0$. It tells us that there are two factors which determine the ion cyclotron oscillation ω: the strength of the electric field $\mathbf{E}$ in which ions are residing, and the initial GC velocity of ions, $\mathbf{v}_{d0}$. If $\mathbf{E} = 0$ and $\mathbf{v}_{d0} = 0$ at the same time, ω returns to Ω; If $\mathbf{E} \neq 0$ but $\mathbf{v}_{d0} = 0$, ω is given by the third expression in Eq.(14) of *Ma & St-Maurice* (2008); If $\mathbf{E} = 0$ but $\mathbf{v}_{d0} \neq 0$, we have $R_{\mathbf{v}} = |\mathbf{v}_{d0}|$, and ω is given by:

$$\omega = \Omega \sqrt{1 + 4 \frac{|\mathbf{v}_{d0}|}{r\Omega}} \neq \Omega \tag{27}$$

which discloses that if ions have a bulk speed in a magnetic field, they will oscillate in a cyclotron frequency which is different from the magnetic gyrofrequency. This is an interesting feature: even though there is no electric field in space, ions can still keep cyclotron oscillations as if they were in an electric field. If $\mathbf{E}$ and $\mathbf{v}_{d0}$ are all nonzero in the case under discussion, we rely on Eq.(26) to calculate ω in a stochastic electric field produced by solitons' space charges.

We are dealing with a case of $\mathbf{v}_{d0} \neq \mathbf{0}$ in the old frame: $\mathbf{v}_{d0} = \{v_{dr0}, v_{d\phi0}\} \neq \mathbf{0}$. Viewed in the new frame, this initial condition is, by using Eq.(19):

$$\mathbf{v}'_{d0} = \{v'_{dr0}, v'_{d\phi0}\} = \{v_{dr0}, v_{d\phi0} - \delta v_\phi\} \neq \mathbf{0} \tag{28}$$

which means that ions start to oscillate from an initial time $t' = t_1$ in the new frame with a nonzero GC velocity vector $\mathbf{v}'_{d0}|_{(t'=t_1)} \neq \mathbf{0}$ which was evolved from $\mathbf{v}'_{d0}|_{(t'=0)} = \mathbf{0}$ in the new frame. The initial time $t' = t_1$ is determined by a relation obtained after applying the initial condition $\mathbf{v}'_{d0}$ to the last two expressions in Eq.(25):

$$\phi_0 = \omega t_1 = -2 \times \tan^{-1} \left(\frac{\omega}{\Omega} \frac{v'_{d\phi0}}{v'_{dr0}} \right) \ , \ \text{or} \ , \ t_1 = -\frac{2}{\omega} \times \tan^{-1} \left(\frac{\omega}{\Omega} \frac{v'_{d\phi0}}{v'_{dr0}} \right) \tag{29}$$

Before the end of this section, we show the expressions of ion bulk kinetic energy $\frac{1}{2} m_i \langle \mathbf{v} \rangle^2$ (where $\langle \mathbf{v} \rangle$ is the ion bulk velocity, or the average velocity) and ion temperature T (hereafter the subscript "$_i$" in T_i is omitted for simplicity) by employing the ion velocity distribution, in order to show the effect of ion cyclotron oscillations on the evolutions of observable ion properties in the stochastic space-charge electric field of solitons.

The ion distribution function f_i under collision-free conditions is obtained from the following Boltzmann equation:

$$\frac{\mathrm{D}f_i}{\mathrm{D}t} = \frac{\partial f_i}{\partial t} + \mathbf{v} \cdot \nabla f_i + \frac{e}{m_i}(\mathbf{E} + \mathbf{v} \times \mathbf{B}) \cdot \nabla_{\mathbf{v}} f_i = 0 \tag{30}$$

in which the electric field $\mathbf{E}$ is "external", produced by the solitons' space charges. Macroscopically, this field is stochastic, maintained by the dynamical processes of the propagation of solitons which are unaffected by the local behavior of the ions; microscopically, within any tiny temporal intervals $(t, t+\Delta t)$ when a specific space-charge electric field appears in space with a lifetime Δt, ions are residing in this "external" constant field from t to $t + \Delta t$. In this sense, we are solving a Boltzmann equation the solution of which can be accessed purely analytically, according to our previous work, rather than a Boltzmann-Vlasov equation (where the electric field in the equation contains both 'external' and 'internal' components) which requires numerical calculations during which the physical mechanism of any resultant effects caused by the stochastic field is more difficult to be recognized.

As discussed in *Ma & St-Maurice* (2008), the function f_i describes the probability of finding a particle (exactly, "an ion" in our case) in a particular volume element $\mathrm{d}\mathbf{r}\mathrm{d}\mathbf{v}$ around the phase-space point $\{\mathbf{r}, \mathbf{v}\}$ in the 6-dimensional phase space filled with identical particles (*Gartenhaus* 1964). Eq.(30) states that in the absence of the short-range collision term $(\partial f_i/\partial t)_{\mathrm{c}}$, f_i remains constant along the 6-dimensional trajectories followed by the ions in phase space, once a particular initial condition is stated (*Schmidt* 1979; *Humphries* 1990). To be more specific, if we know the initial ion distribution function at an initial phase-space vector point $\{\mathbf{r}(t_0), \mathbf{v}(t_0)\} = \{\mathbf{r}_0, \mathbf{v}_0\}$ in any tiny temporal intervals, we are able to describe the ions' distribution function $f_i(\mathbf{r}, \mathbf{v}, t)$ at any time in the intervals in phase space, namely, the problem $Df_i/Dt = 0$ is simply formally given by

$$f_i(\mathbf{r}, \mathbf{v}, t) = f_i(\mathbf{r}_0, \mathbf{v}_0, t_0) = f_0(r_0, v_{r0}, v_{\phi 0}, t_0) \tag{31}$$

Let n_i represent ion density, and $T = \{T_r, T_\phi, T_\parallel\}$ represent the temperature where T_r, T_ϕ, and $T_\parallel$ are the three components in radial, azimuthal, and axial directions, respectively. By assuming that the initial distribution f_0 of ions is a time-stationary, position-independent, velocity-shifted, density-homogeneous, and temperature-anisotropic Maxwellian with nonzero initial GC velocity $\mathbf{v}_{\mathrm{d}0}$, initial temperature $T_{r0} = T_{\phi 0} = T_\parallel = T_0$, initial density n_0, and initial time $t_0 = 0$, we have:

$$f_0 = \frac{n_0 m_i}{2\pi k_b T_0} \exp\left[-\frac{m_i[(v_{r0} - v_{\mathrm{d}r0})^2 + (v_{\phi 0} - v_{\mathrm{d}\phi 0})^2]}{2k_b T_0} \right] \tag{32}$$

Here, we employ a "Backward mapping" approach to transform this initial distribution f_0 to the final solution of the Boltzmann equations. As introduced in details Ma & St.-Maurice (2008, 2015), the core of this approach lies in the task of finding an explicit connection between the initial phase-space state, $\{\mathbf{r}_0, \mathbf{v}_0, t_0\}$, and the final one, $\{\mathbf{r}, \mathbf{v}, t\}$. Luckily, this relation can be obtained if we solve the set of differential equations of motion as done in Ma & St.-Maurice (2008): there are two identical solutions for the same set of equations of motion (Gartenhaus 1964): one provides $\{\mathbf{r}, \mathbf{v}, t\}$ expressed by using $\{\mathbf{r}_0, \mathbf{v}_0, t_0\}$ (*forward mapping*), while the other provides $\{\mathbf{r}_0, \mathbf{v}_0, t_0\}$ expressed by using $\{\mathbf{r}, \mathbf{v}, t\}$ (*backward mapping*), whereby the description of the characteristics of motion is traced backwards but is otherwise unaltered. We use the latter method to solve $f_i(\mathbf{r}, \mathbf{v}, t)$. This method allows us to relate the 6-dimensional phase point $\{\mathbf{r}, \mathbf{v}\}$ at any time t to $\{\mathbf{r}_0, \mathbf{v}_0, t_0\}$ and to therefore find the distribution at time t, since the initial distribution is already fully known, as given by Eq.(32). Finding the distribution function is then just a matter of expressing $\mathbf{r}_0$ and $\mathbf{v}_0$ in terms of $\mathbf{r}, \mathbf{v}$, and t in the expression for the initial condition f_0. Therefore, Eqs.(12,31) thus give

$$f_i(r, v_r, v_\phi, t) = \frac{\left(\frac{a_{00}}{a_0} n_0\right) m_i}{2\pi k_b \left(\frac{a_{00}}{a_0} T_{i0}\right)} \exp\left[-\frac{m_i[(v_r - v_{\mathrm{d}r})^2 + (v_\phi - v_{\mathrm{d}\phi})^2]}{2k_b \left(\frac{a_{00}}{a_0} T_{i0}\right)} \right] \tag{33}$$

from which we have n_i, average velocity $\langle \mathbf{v} \rangle = \{\langle v_r \rangle, \langle v_\phi \rangle\}$, and T as follows:

$$\frac{n_i}{n_0} = \frac{T_r}{T_0} = \frac{T_\phi}{T_0} = \frac{a_{00}}{a_0} \ , \quad \langle \mathbf{v} \rangle = \mathbf{v}_{\mathrm{d}} = \{v_{\mathrm{d}r}, v_{\mathrm{d}\phi}\} \tag{34}$$

Consequently, the ion bulk kinetic energy $\frac{1}{2}m_i\langle\mathbf{v}\rangle^2$ and temperature T are expressed by

$$\frac{1}{2}m_i\langle\mathbf{v}\rangle^2 = \frac{1}{2}m_i\mathbf{v}_{\mathrm{d}}^2 \ , \quad T_i = \frac{T_r + T_\phi + T_\parallel}{3} = T_0\frac{2\frac{a_{00}}{a_0}+1}{3} \tag{35}$$

in which $\mathbf{v}_{\mathrm{d}}^2 = v_{\mathrm{d}r}^2 + v_{\mathrm{d}\phi}^2$. In dimensionless forms with T_i normalized by T_0, $v_{\mathrm{d}r}$ & $v_{\mathrm{d}\phi}$ by v_{th} (the ion thermal equilibrium speed), and thus $\frac{1}{2}m_i\langle\mathbf{v}\rangle^2$ & $\frac{1}{2}m_i\mathbf{v}_{\mathrm{d}}^2$ by $\frac{1}{2}m_i v_{th}^2$, Eq.(35) becomes

$$\langle\mathbf{v}\rangle^2 = \mathbf{v}_{\mathrm{d}}^2 \ , \quad T_i = \frac{2\frac{a_{00}}{a_0}+1}{3} \tag{36}$$

4 Oscillations in a stochastic nonlinear wavefield

In a period of time 1 s, we artificially choose ten random electric field strengths of E_r to produce ten E_c/B values at ten random moments t_i ($i = 1 \sim 10$) in sequence, as shown in Column A and B, respectively, in Table 1. Column C gives $(E_c/B)(r/R_c)$ at $r = 0.5R_c$. Hereafter, the subscript numbers from 1 to 10 attached to all physical parameters indicate the corresponding E_r-levels, respectively.

Table 1. Parameters of Stochastic heating or acceleration by 10 Random Potential Wells in $0 \sim 1$ s at $r/R_0 = 0.5$

	A	B	C	D	E	F	G	H	I	J	K	L
Level	t_i(s)	E_c/B	$\frac{E_c}{B}\frac{r}{R_c}$	$v_{\mathrm{d}r}(t_i)$	$v_{\mathrm{d}\phi}(t_i)$	R_v	ω/Ω	δv_ϕ	ϕ_0(rad)	$a_0(t_i)$	a_{00}	$1/a_{00}$
1	0	2.0	1	0	0	1	1.915	0	0	1	1	1
2	0.05	3.6	1.80	-0.060	0.002	1.799	2.408	0.001	0.080	0.998	0.999	1.001
3	0.13	0.2	0.10	-1.051	0.340	1.078	1.969	-0.978	2.372	0.688	1.897	0.527
4	0.21	1.5	0.75	.358	-0.917	1.705	2.355	-0.955	-0.490	1.754	1.843	0.543
5	0.23	0.0	0.00	-0.811	-0.750	1.104	1.986	-1.104	1.430	1.447	2.131	0.469
6	0.30	1.0	0.50	0.474	-0.997	1.571	2.278	-1.071	-0.677	1.865	2.047	0.489
7	0.46	2.8	1.40	-1.360	-0.286	2.166	2.603	-0.776	1.486	1.001	1.641	0.609
8	0.69	0.7	0.35	0.978	-0.532	1.318	2.125	-0.968	-1.541	1.251	1.977	0.506
9	0.83	4.5	2.25	0.155	-0.959	3.212	3.093	-0.962	-0.149	1.953	1.963	0.509
10	0.92	0	0	-2.047	-0.225	2.060	2.548	-2	2.291	0.990	3.323	0.301
END	1	0	0	-2.047	-0.225	2.060	2.548	-2	2.291	0.990	3.323	0.301

4.1 E_r-level 1 in $t \in [t_1, t_2]$: Initial oscillations with ω_1

Before $t < 0$, ions are assumed at the state of a thermal equilibrium in the absence of any electric field with $\mathbf{v}_{\mathrm{d}}|_{t<0} = \{v_{\mathrm{d}r}, v_{\mathrm{d}\phi}\}|_{t<0} = \{0, 0\} = \mathbf{0}$.

At $t = t_1 = 0$, Level 1 begins with E_{c1}/B switched on. It lasts from t_1 to $t_2 = 0.05$ s: $t \in [t_1, t_2]$. The initial conditions are as follows: $a_{01}(t_1) = a_{001}(t_1) = a_{001}^{-1}(t_1) = 1$, $v_{\mathrm{d}r1}(t_1) = v_{\mathrm{d}r}|_{t<0} = 0$, and $v_{\mathrm{d}\phi1}(t_1) = v_{\mathrm{d}\phi}|_{t<0} = 0$, along with $\delta v_{\phi1} = \phi_{01} = 0$. This is the case described in great details in *Ma & St-Maurice* (2008) when the $\mathbf{v}_{\mathrm{d}}$-circle passes through the origin. The input parameters of this level are as follows:

$$\left.\begin{aligned}
R_{\mathbf{v}1} &= \sqrt{[v_{\mathrm{d}r1}(t_1)]^2 + \left[v_{\mathrm{d}\phi1}(t_1) - \frac{E_{c1}}{B}\frac{r}{R_c}\right]^2} = \frac{E_{c1}}{B}\frac{r}{R_c} \\
\frac{\omega_1}{\Omega} &= \sqrt{1 + 4\frac{E_{c1}/B}{R_c\Omega}} = \sqrt{1 + \left(4\frac{R_c}{r}\right)\frac{R_{\mathbf{v}1}}{R_c\Omega}} = \sqrt{1 + 8\frac{R_{\mathbf{v}1}}{R_c\Omega}} \\
\delta v_{\phi1} &= \frac{E_{c1}}{B}\frac{r}{R_c} - R_{\mathbf{v}1} = 0 \\
\phi_{01} &= -2\tan^{-1}\left[\frac{\omega_1}{\Omega}\frac{v_{\mathrm{d}\phi1}(t_1)-\delta v_{\phi1}}{v_{\mathrm{d}r1}(t_1)}\right]\Big|_{(v_{\mathrm{d}r1}\to 0)} = 0 \\
\frac{a_{01}(t_1)}{a_{001}} &= 1 - \frac{1}{2}\left[1 - \left(\frac{\Omega}{\omega_1}\right)^2\right](1-\cos\phi_{01}) = 1 \\
a_{001} &= a_{01}(t_1)/\left[\frac{a_{01}(t_1)}{a_{001}}\right]
\end{aligned}\right\} \tag{37}$$

Notice that the ion cyclotron oscillation frequency ω is written in its genuine form: it is as a matter of fact determined by $R_{\mathbf{v}}$, rather than E_c/B; however, if the initial ion GC velocity $\mathbf{v}_{\mathrm{d}}$ is zero, we have $R_{\mathbf{v}} = E_c/B$ (a case discussed in *Ma & St-Maurice* 2008).

In $t \in (t_1, t_2)$, these input parameters give rise to the ion characteristics of motion at an arbitrary time t as follows:

$$
\left.
\begin{aligned}
\frac{a_{01}(t)}{a_{001}} &= 1 - \frac{1}{2}\left[1 - \left(\frac{\Omega}{\omega_1}\right)^2\right]\{1 - \cos[\omega_1(t - t_1) + \phi_{01}]\} \\
a_{01}(t) &= a_{001} \cdot \left[\frac{a_{01}(t)}{a_{001}}\right] \\
v_{\mathrm{d}r1}(t) &= -R_{\mathbf{v}1}\left[\frac{a_{01}(t)}{a_{001}}\right]^{-1}\frac{\Omega}{\omega_1}\sin[\omega_1(t - t_1) + \phi_{01}] \\
v_{\mathrm{d}\phi1}(t) &= R_{\mathbf{v}1}\left[\frac{a_{01}(t)}{a_{001}}\right]^{-1}\left(\frac{\Omega}{\omega_1}\right)^2\{1 - \cos[\omega_1(t - t_1) + \phi_{01}]\} + \delta v_{\phi1}
\end{aligned}
\right\}
\tag{38}
$$

At the end of the stage, $t = t_2$, above functions have following values, respectively:

$$
\left.
\begin{aligned}
\frac{a_{01}(t_2)}{a_{001}} &= 1 - \frac{1}{2}\left[1 - \left(\frac{\Omega}{\omega_1}\right)^2\right]\{1 - \cos[\omega_1(t_2 - t_1) + \phi_{01}]\} \\
a_{01}(t_2) &= a_{001} \cdot \left[\frac{a_{01}(t_2)}{a_{001}}\right] \\
v_{\mathrm{d}r1}(t_2) &= -R_{\mathbf{v}1}\left[\frac{a_{01}(t_2)}{a_{001}}\right]^{-1}\frac{\Omega}{\omega_1}\sin[\omega_1(t_2 - t_1) + \phi_{01}] \\
v_{\mathrm{d}\phi1}(t_2) &= R_{\mathbf{v}1}\left[\frac{a_{01}(t_2)}{a_{001}}\right]^{-1}\left(\frac{\Omega}{\omega_1}\right)^2\{1 - \cos[\omega_1(t_2 - t_1) + \phi_{01}]\} + \delta v_{\phi1}
\end{aligned}
\right\}
\tag{39}
$$

We know that $a_{01}(t_2)$ and $\{v_{\mathrm{d}r1}(t_2), v_{\mathrm{d}\phi1}(t_2)\}$ represent the ion temperature and GC velocity at $t = t_2$, respectively. They keep invariant during the switch of the electric field from level 1 to 2:

$$
a_{02}(t_2) = a_{01}(t_2) \ , \ v_{\mathrm{d}r2}(t_2) = v_{\mathrm{d}r1}(t_2) \ , \ v_{\mathrm{d}\phi2}(t_2) = v_{\mathrm{d}\phi1}(t_2)
\tag{40}
$$

4.2 E_r-level 2 in $t \in [t_2, t_3]$: Oscillations with ω_2 for generalization

Without loss of generality, we give expressions for the ion oscillation features at this level after the electric field switches from E_{c1}/B to E_{c2}/B. By using the initial conditions given by Eq.(40), we obtain the input parameters as follows:

$$
\left.
\begin{aligned}
R_{\mathbf{v}2} &= \sqrt{\left[v_{\mathrm{d}r2}(t_2)\right]^2 + \left[v_{\mathrm{d}\phi2}(t_2) - \frac{E_{c2}}{B}\frac{r}{R_c}\right]^2} \\
\frac{\omega_2}{\Omega} &= \sqrt{1 + 8\frac{R_{\mathbf{v}2}}{R_c\Omega}} \\
\delta v_{\phi2} &= \frac{E_{c2}}{B}\frac{r}{R_c} - R_{\mathbf{v}2} \\
\phi_{02} &= -2\tan^{-1}\left[\frac{\omega_2}{\Omega}\frac{v_{\mathrm{d}\phi2}(t_2) - \delta v_{\phi2}}{v_{\mathrm{d}r2}(t_2)}\right] \\
\frac{a_{02}(t_2)}{a_{002}} &= 1 - \frac{1}{2}\left[1 - \left(\frac{\Omega}{\omega_2}\right)^2\right](1 - \cos\phi_{02}) \\
a_{002} &= a_{02}(t_2)/\left[\frac{a_{02}(t_2)}{a_{002}}\right]
\end{aligned}
\right\}
\tag{41}
$$

which gives rise to the ion characteristics of motion at an arbitrary time t as follows:

$$
\left.
\begin{aligned}
\frac{a_{02}(t)}{a_{002}} &= 1 - \frac{1}{2}\left[1 - \left(\frac{\Omega}{\omega_2}\right)^2\right]\{1 - \cos[\omega_2(t - t_2) + \phi_{02}]\} \\
a_{02}(t) &= a_{002} \cdot \left[\frac{a_{02}(t)}{a_{002}}\right] \\
v_{\mathrm{d}r2}(t) &= -R_{\mathbf{v}2}\left[\frac{a_{02}(t)}{a_{002}}\right]^{-1}\frac{\Omega}{\omega_2} \cdot \sin[\omega_2(t - t_2) + \phi_{02}] \\
v_{\mathrm{d}\phi2}(t) &= R_{\mathbf{v}2}\left[\frac{a_{02}(t)}{a_{002}}\right]^{-1}\left(\frac{\Omega}{\omega_2}\right)^2\{1 - \cos[\omega_2(t - t_2) + \phi_{02}]\} + \delta v_{\phi2}
\end{aligned}
\right\}
\tag{42}
$$

At the end of the stage, $t = t_3$, above functions have following values, respectively:

$$\left.\begin{array}{l} \frac{a_{02}(t_3)}{a_{002}} = 1 - \frac{1}{2}\left[1 - \left(\frac{\Omega}{\omega_2}\right)^2\right]\{1 - \cos[\omega_2(t_3 - t_2) + \phi_{02}]\} \\[2mm] a_{02}(t_3) = a_{002} \cdot \left[\frac{a_{02}(t_3)}{a_{002}}\right] \\[2mm] v_{\mathrm{d}r2}(t_3) = -R_{\mathbf{v}2}\left[\frac{a_{02}(t_3)}{a_{002}}\right]^{-1}\frac{\Omega}{\omega_2}\sin[\omega_2(t_3 - t_2) + \phi_{02}] \\[2mm] v_{\mathrm{d}\phi2}(t_3) = R_{\mathbf{v}2}\left[\frac{a_{02}(t_3)}{a_{002}}\right]^{-1}\left(\frac{\Omega}{\omega_2}\right)^2\{1 - \cos[\omega_2(t_3 - t_2) + \phi_{02}]\} + \delta v_{\phi2} \end{array}\right\} \qquad (43)$$

which keep invariant during the switch of the electric field from level 2 to 3, and behave as the initial conditions for the new step:

$$a_{03}(t_3) = a_{02}(t_3) \ , \ v_{\mathrm{d}r3}(t_3) = v_{\mathrm{d}r2}(t_3) \ , \ v_{\mathrm{d}\phi3}(t_3) = v_{\mathrm{d}\phi2}(t_3) \qquad (44)$$

4.3   All E_r-levels: Oscillations with different cyclotron frequencies

By generalizing expressions given above with reiterations of similar derivations, we calculate $v_{\mathrm{d}r}$, $v_{\mathrm{d}\phi}$, R_{v}, ω/Ω, δv_ϕ, ϕ_0, $a_0(t_i)$, a_{00}, and a_{00}^{-1} for all E_r-levels. Data are given in columns $D \sim L$, respectively, of Table 1. The temporal changes of these parameters are depicted in Figs. 3~5. From the evolutions of the parameters in these figures, we see several oscillation features of ions as follows.

First of all, any random change in E_c/B causes immediate variations in other parameters. For example, in the upper left panel of Fig.3, when $\frac{E_c}{B}\frac{r}{R_c}$ increases from 1 to 1.8 at $t = 0.05$ s followed by a drop to 0.1 at $t = 0.13$ s, ω/Ω in the lower left panel goes up from 1.915 to 2.408, and then decreases to 1.969 without any delay. Accordingly, other parameters (e.g., R_{v}, δv_ϕ, a_{00}) also have prompt jumps.

Secondly, though solitons' electric field stimulates ions from the gyration frequency Ω to the stochastic cyclotron frequency ω, ω never returns to Ω even if the electric field is turned off. Look at E_r-level 5 and 10 in the upper left panel of Fig.3, where the electric field strengths are zero. However, the ω/Ω-values in the lower left panel are 1.986 and 2.548, respectively, not 1 (or, $\omega = \Omega$) as normally considered it should be in the absence of electric fields. This indicates that when the electric field disappears, ions still oscillate as if there were an electric field. As discussed in the last section, this "imaginary" field is nothing but as a matter of fact a reflection of the nonzero drift velocity that ions have acquired before the electric field is off.

Thirdly, during the stochastic cyclotron oscillations, ions are heated transversely, as revealed by the evolution of $a_0^{-1}(t)$ in Fig.4. As discussed in the last section, $a_0^{-1}(t)$ reflects the ions' transverse temperature T_r (or T_ϕ) evolving from the initial isothermal T_0 in the soliton's space-charge electric field proportional to the radius. Fig.4 shows that $a_0^{-1}(t)$ is mostly higher than 1. This means that T is often above T_0. The figure shows that ions are heated to 1.36 T_0 on average, changing from $0.3T_0$ to $5.8T_0$, while Table 1 tells us that ω varies from 1.915Ω to 3.093Ω during this period of time. Thus, cyclotron oscillations and transverse ion heating are the both available manifestations of the presence of the solitons, or, exactly, their space-charge electric field in space at any time. It is worth to mention here that the last two columns a_{00} and a_{00}^{-1} in Table 1 are retrospective values of $a_0(t)$ and $a_0^{-1}(t)$, respectively, at $t_i' = 0$ in the shifted frame with the origin O'.

Lastly, in sharp contrast to the random amplitudes of $v_{\mathrm{d}r}(t_i)$ and $v_{\mathrm{d}\phi}(t_i)$ caused by the electric field switches, as shown in the upper right panel of Fig.3, the GC-velocity (or, the $\mathbf{v}_{\mathrm{d}}$-vector) evolves in circles with different radii in velocity space during these switches, as shown in Fig.5. All the $\mathbf{v}_{\mathrm{d}}$-circles are symmetric to the axis of $v_{\mathrm{d}r}(t)$=0. This means that the mean amplitude of $v_{\mathrm{d}r}(t)$ is always zero. Thus, $\mathbf{v}_{\mathrm{d}}$ rotates in ϕ-direction on average with a temporally changing speed, as shown by, e.g., Eq.(42).
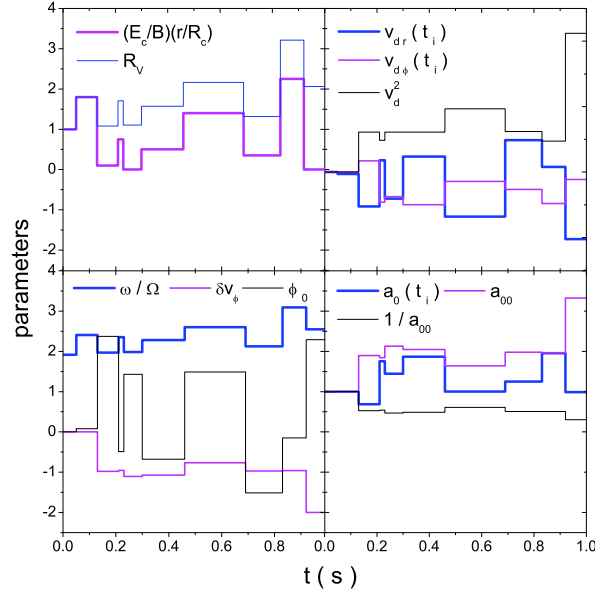
Fig. 3 Evolution of parameters in response to artificially generated stochastic electric fields of solitons. Data are given in Table 1. **E**=0 is set initially before $t = 0$, at level 5 of $0.23 < t < 0.3$, and finally after $t > 0.92$ s.
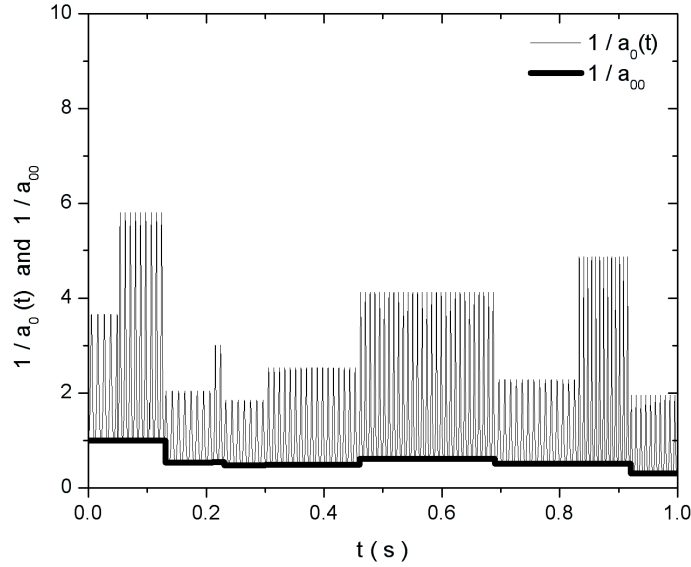

Fig. 4 Evolution of $a_0^{-1}(t)$ and a_{00}^{-1} in response to artificially generated stochastic electric fields of solitons.

5   Oscillations in a generalized stochastic nonlinear wavefield

In order to get deeper insights into the features of the ion cyclotron oscillations triggered by stochastic space-charge electric fields of solitons, we use two random-number generators to simulate the stochastic
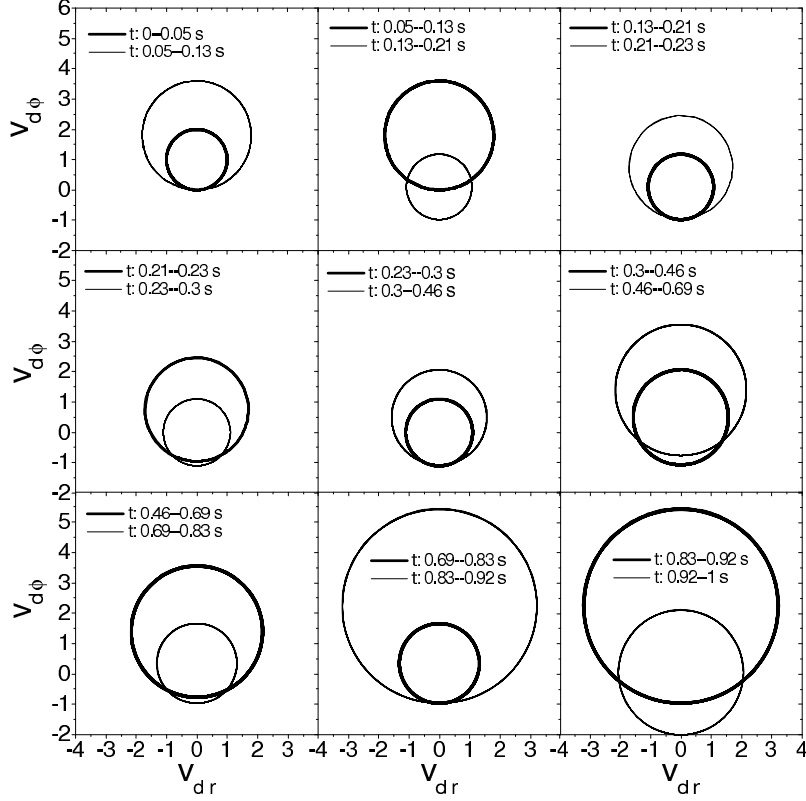
Fig. 5 GC-velocity $\mathbf{v}_d$-circles in response to the artificially generated stochastic electric field of solitons.

appearances and the E_c/B strengths of electron solitons. The maximum temporal interval is 1 (in unit of one gyro-period $2\pi/\Omega$ s). The lifespan of the stochastic electric field is 4000 gyro-periods. The calculation also gives results for extra 1000 gyro-periods to see what happens after the electric field is switched off. We consider ions at $r = 0.5R_c$.

For comparisons, we consider both a low-amplitude stochastic electric field of solitons and a high-amplitude one, corresponding to two extreme cases FAST could encountered. The peak E_c/B-strength in the former is 4 (in unit of $v_{th} = 1$ km/s), while $R_c\Omega = 3$ (in unit of v_{th}); by contrast, the peak E_c/B-strength in the latter is 90, while $R_c\Omega = 275$. The two corresponding nominal ion gyration frequencies (that for Maxwellian ions with zero GC velocity to response to the peak stochastic electric field strength) are 2.52Ω and 1.52Ω, respectively.

Fig.6 illustrates the oscillating properties of following four parameters with time in the low-amplitude stochastic field: $(E_c/B)(r/R_c)$, R_v, δv_ϕ, and ω/Ω. The upper left panel gives the input stochastic $(E_c/B)(r/R_c)$-profile which is zero after $t = 4000$. The upper right panel shows the stochastic changes of the velocity radius of the GC-circles, R_v. Although $\frac{E_c}{B}\frac{r}{R_c}$ never exceeds 2, it can reach up to more than 25 in modulations. From $t = 4000$, it is fixed at about 23. The lower left panel presents the variations of the shift between the old coordinates and a series of new ones in the stochastic electric field, δv_ϕ. Because this shift is equal to $(\frac{E_c}{B}\frac{r}{R_c} - R_v)$, it has an anti-correlation with R_v due to relatively small amplitudes of $\frac{E_c}{B}\frac{r}{R_c}$ at any time. The lower right panel exhibits the evolving properties of the ion cyclotron frequency ω. Obviously, it is positively correlated to R_v, in agreement with what was discussed in the last Section. It is within $1 \sim 9\Omega$ in frequencies but with an average around $\sim 5.5\Omega$. Note that the final oscillation is frozen at 8Ω after 4000 gyro-periods of time when the electric field is switched off.
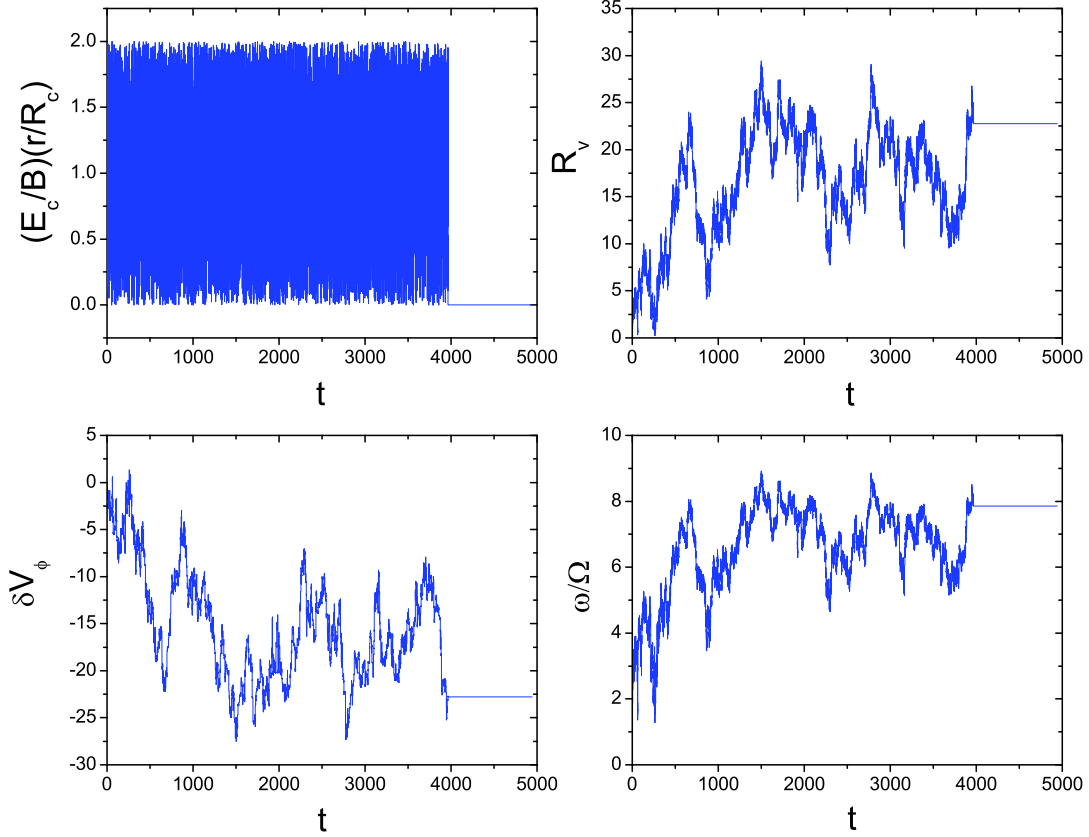
Fig. 6 Oscillations of four parameters with time in a low-amplitude stochastic space-charge electric field of solitons: $(E_c/B)(r/R_c)$, R_v, δv_ϕ, and ω/Ω.

Fig.7 displays the temporal evolutions of the transverse GC kinetic energy v_d^2 (in unit of v_{th}^2) of ions and their temperature T (in unit of T_0) in this case. The upper panel shows that that the kinetic energy is enhanced by at least 2 orders of magnitude by the stochastic electric field. For the ion temperature, it also demonstrate markedly up to a 20-fold increase. Because in the present study the the parallel component is assumed constant, the temperature growth is contributed by the transverse components T_r and T_ϕ. After 4000 gyrations of time, both v_d^2 and T keep constant in time, much higher than their respective initial values.

Fig.8 and Fig.9 manifest the four parameters and v_d^2 & T, respectively, in the high-amplitude stochastic field. From the upper left panel of Fig.8, we see that $(E_c/B)(r/R_c)$ is much higher than that in Fig.6, which produces much higher R_v, δv_ϕ. On the contrary, the cyclotron frequency ω in the lower right panel of Fig.8 is lower than that in Fig.6. By checking analytical expressions in the last section, we know that ω/Ω is really related to the electric field (E_c/B), but depends on the ratio between (E_c/B) and $R_c\Omega$. Though (E_c/B) increases 22.5 times the weak field, the fact that $R_c\Omega$ becomes 91 times the weak field makes the ratio is smaller than that in the weak field. Thus, ω has smaller amplitudes which are within $1 \sim 7\Omega$ in frequencies. The average is around $\sim 4.4\Omega$ which seems to be the final value stabilized after 4000 gyro-periods of time. Strikingly, the gained kinetic energy of ions is much higher in Fig.9 than that in Fig.7, while the ion temperature shown in Fig.9 does not increase that much as that in Fig.7.
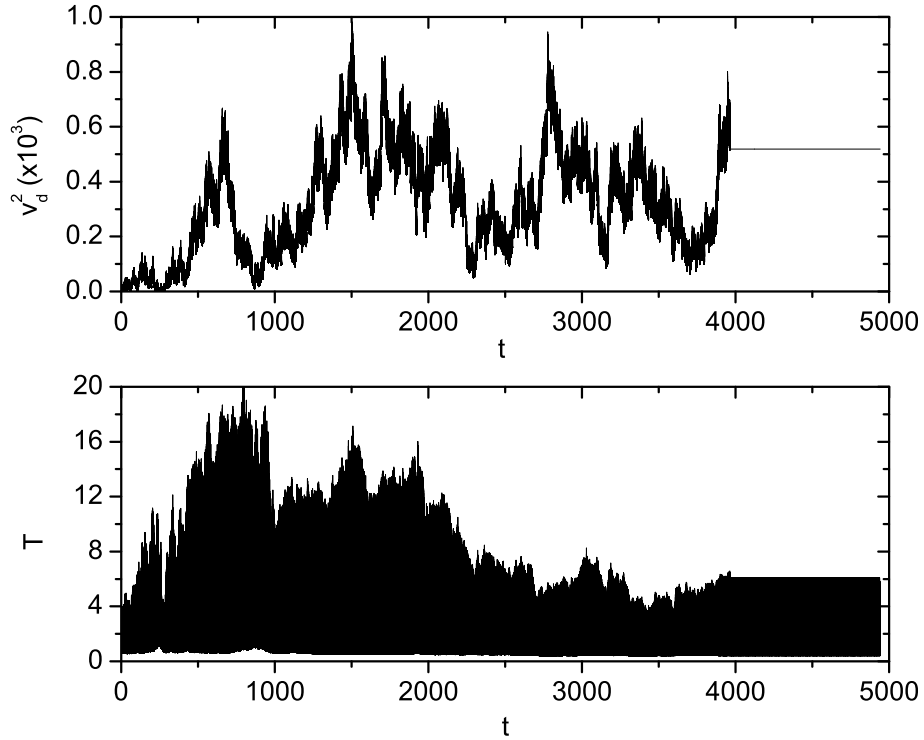
Fig. 7   Temporal evolutions of the transverse GC kinetic energy $v_{\rm d}^2$ of ions and their temperature T in a low-amplitude stochastic space-charge electric field of solitons.

For the two cases, the IC oscillation frequency shifts around $\sim 5\Omega$ on average, between 4.4Ω and 5.5Ω. This indicate that observable frequencies should not fall exactly about Ω. Instead, they should be away from the ion gyro-frequency. In the present radially inward electric field case, ω has a "blue" shift to the LH frequency. Reasonably, if the electric field is radially outward (say, produced by positive space-charge solitons), we predict ω will have a "red" shift to a frequency lower than Ω. Another paper will discuss this case.

6   Summary and discussion

Plasma instabilities and waves in IC modes is a hot topic in traditional linear wave theories, where the electric field is weak, considered as a perturbation under a plane wave formulation. Aiming at illustrating the IC oscillations in response to a stochastic, strong electric field contributed by nonlinear waves in auroral ionosphere, we established a physical model to describe characteristics of ions residing in such an electric field which randomly appears in space with random strengths, however, is instantaneously constant in time. To get easy access and comprehensive insight into the oscillation features, we relied on ion Hamiltonian mechanics to solve the Boltzmann equation completely analytically for an invariant field with time. We obtained a double-circle trajectory in velocity space for ions with a nonzero initial GC velocity, and acquired evolutions of their kinetic energy and temperature. Then, we designed a stochastic electric field with 10-step strengths to illustrate how the IC oscillation frequency and other parameters accommodate to the strong space-charge electric field of solitons which appears in flux tubes randomly with time. After that, we bring two random-number generators into play to simulate real situations at a position well inside the flux tube. We obtained that the IC frequency can be shifted
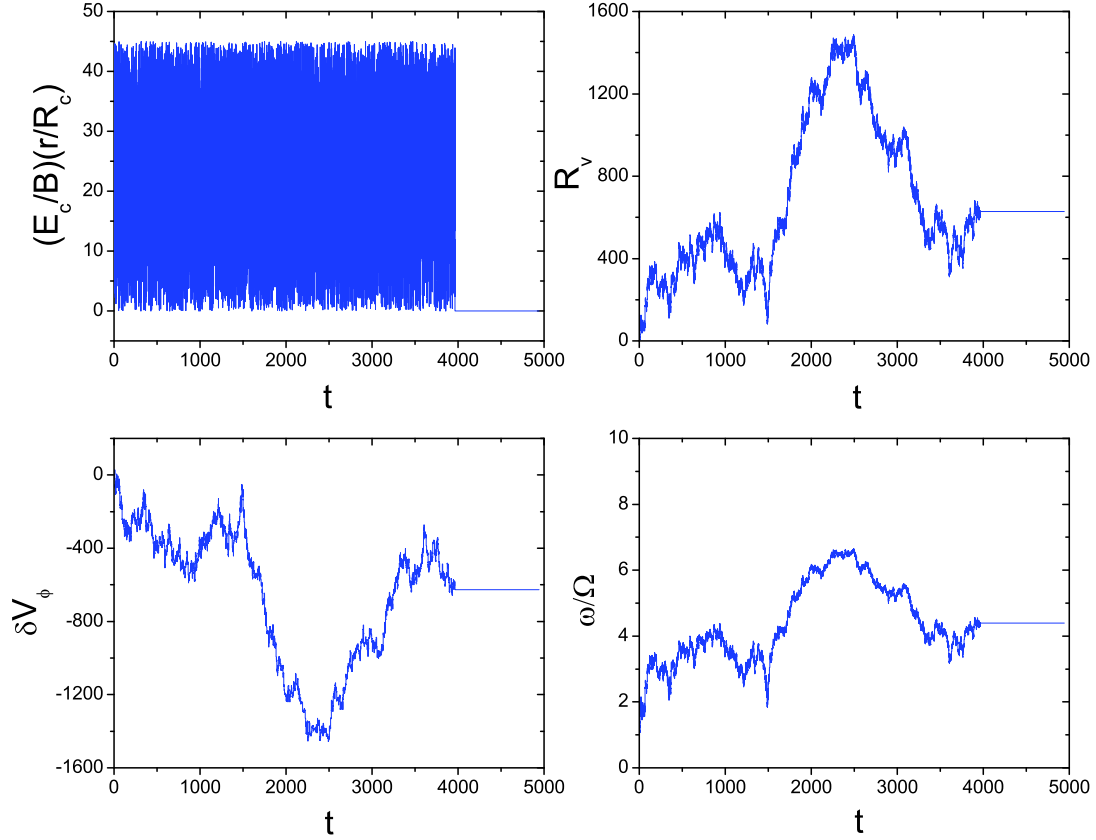
Fig. 8 Oscillations of four parameters with time in a high-amplitude stochastic space-charge electric field of solitons: $(E_c/B)(r/R_c)$, R_v, δv_ϕ, and ω/Ω.

to several ion gyration frequencies. Specifically, with both a low-amplitude electric field and a high-amplitude one, we reported that the actual IC frequencies fall in around 5Ω on average of the two cases.

The simulation result coincides with observations, e.g., FAST data. See Fig.1(aa-cc) in *Ergun et al.* (1998c). The data gives five pulses in ~ 5 ms, indicating a frequency of ~ 1 kHz for solitary structures to appear at a specific spatial position. Using H^+ gyrofrequency $\Omega \sim 200$ Hz we calculated in Section 1 from FAST measurements, we predicted from our result that solitons should have a frequency of $880 \sim 1100$ Hz, in agreement with what FAST data exhibited. Here, we would like to show our special concern to the authors' claim that the frequency of the evenly spaced solitons appears to be, "within error", the LH oscillations (see Fig.5 in that paper). In the linear wave regime, the LH instabilities are triggered by the density and/or temperature gradients of the background plasma, involving both modulations of the perturbed electric field to electrons and ions. In upward/downward current regions FAST satellite passes, such conditions to excite LH waves seem not satisfied in the linear wave regime. If LH oscillations do exist, they may be triggered by some kind of mechanisms related to strong soliton electric fields. Unfortunately, the authors mentioned nothing about the activation of the LH instabilities. We are going to pay attention to this issue and show linked evidence to support the authors' argument.

This paper is the first attempt to account for measurements of plasma IC oscillations by employing a nonlinear plasma wave model. The approach hires the kinetic theory, instead of the linear wave theory,
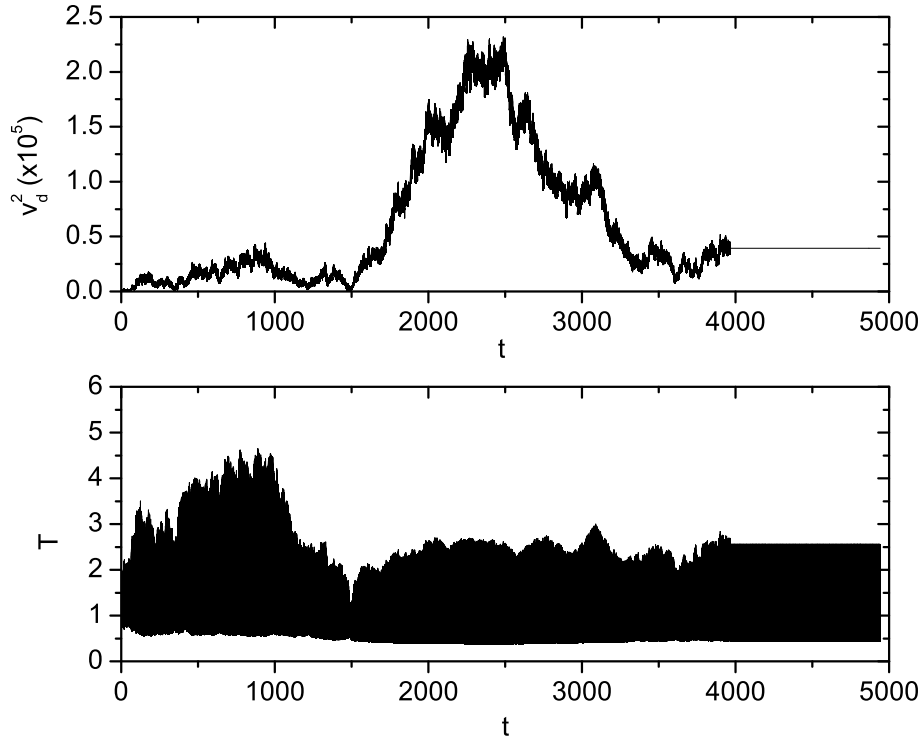
Fig. 9   Temporal evolutions of the transverse GC kinetic energy v_{d}^2 of ions and their temperature T in a high-amplitude stochastic space-charge electric field of solitons.

to understand the IC oscillations observed in space, where the linear plasma process has evolved to produce measurable nonlinear phenomena by high-resolution payloads. As a start, we attacked the most basic problem with as simple a model as possible toward our goal to gain important insights into more complicated situations, while still being able to obtain applicable numerical solutions to observations. In the model, we did not take into consideration the effect of the parallel electric field sustained by solitons on perpendicular ion oscillations, and neglected an upward mirror force which may be brought about by a diverging magnetic flux tube. We exclude the boundary effects on the characteristics of ions by simply choosing a radius which is well inside the flux tube cylinder. We also assumed that the solitons' space charges are distributed in the flux tube uniformly, regardless of a possible density inhomogeneity due to intermediate spaces among soliton trains. Though with these limits, the feature of measured IC oscillations driven by nonlinear waves can be satisfactorily explained. We hope the work could provide a reference to future studies on solving similar problems under conditions that traditional linear wave models are no longer suitable.

7   Conclusion

After Chiueh & Diamond predicted the existence of "space-charge Clumps, numerous high-resolution observations (e.g., FAST, Polar) confirmed these space-charge structures which were nothing else but the measured nonlinear electrostatic solitary waves (see the first report by Matsumoto et al. 1994). These stochastic solitary structures are space-charge carriers which contribute strong transverse electric fields in space plasmas to excite ion cyclotron (IC) oscillations. Different from the stochastic methods used in different fields of physics (Bonfig 1988; Vojko et al. 1994; Vojko & Dali 1996), this paper offered an alternative for readers to deal with similar studies in the elucidation of the IC oscillations stimulated

in auroral ionosphere. This new approach was featured by a couple of recognitions in treating the space-charge electric field, as demonstrated by *Ma et al.* (2009): macroscopically, the field is stochastic, maintained by the dynamical processes of the propagation of solitons unaffected by the local behaviour of the ions; microscopically, within any tiny temporal intervals when a specific space-charge electric field appears in space with a lifetime ions are residing in this externally constant field. In that sense, we are solving a simpler Boltzmann equation analytically, rather than a more complicated Boltzmann-Vlasov equation which requires numerical approaches. For the stochastic, strong space-charge electric wavefield $\mathbf{E}$ of nonlinear waves propagating in auroral ionosphere, we conclude that

(1) With a nonzero initial guiding-center (GC) velocity, ions are found to follow a double-circle trajectory in velocity space with an IC oscillation frequency ω which shifts from the magnetic gyrofrequency $\Omega = eB/m_i$;

(2) After the "constant" condition of the field is relaxed by using a simple stochastic $\mathbf{E}$ strengths in different limited random time intervals, frequency ω accommodates the $\mathbf{E}$ switches which brings about variations of related transport parameters;

(3) By generalizing the stochastic properties in both the field strength and time interval, ω can be shifted to several times over the value of Ω, bringing astonishing enhancements in the physical properties such as, temperature, kinetic energy, in good agreement with what observations demonstrated in auroral field-aligned current regions.

References

Bale S D, Kellogg P J, Larson D E, et al 1998 *Geophys. Res. Lett.*, **25**, 2929–32

Barkan A, D'Angelo N and Merlino R L 1995 *Planet. Space Sci.*, **43**(7), 905–8

Bernstein I B, Green J M and Kruskal M D 1957 *Phys. Rev.*, **108**, 546–50

Bernstein I B 1958 *Phys. Rev.*, **109**(1), 10–21

Boardsen S A, Gurnett D A, and Peterson W K 1990 *J. Geophys. Res.*, **95**, 10,591-8.

Bonfig K W 1988 *Sensors*, **3**, 103–8

Boström R, Gustafsson G, Holback B, et al 1988 *Phys. Rev. Lett.*, **61**, 82–5

Bounds S R, Pfaff R F, Knowlton S F, et al 1999 *J. Geophys. Res.*, **104**, 28709–17

Büchner J and Elkina N 2006 *Phys. Plasmas*, **13**, 082304

Cattell C A, Mozer F S, Anderson R R, et al 1986 *J. Geophys. Res.*, **91**, 5681–8

Cattell C A, Dombeck J, Wygant J R, et al 1999 *Geophys. Res. Lett.*, **26**, 425–8

Chaston C C, Bonnell J W, McFadden J P, et al 2002 *J. Geophys. Res.*, **107**(A11), SMP 8.1–19

Chiueh T and Diamond P H 1986 *Phys. Fluids*, **29**(1), 76–96

Chow V W and Rosenberg M 1995 *Planet. Space Sci.*, **43**(5), 613–8

Chow V W and Rosenberg M 1996 *Phys. Plasmas*, **3**(4), 1202–11

Cole K D 1976 *Planet. Space Sci.*, **24**, 515–8

D'Angelo N and Motley R W 1962 *Phys. Fluids*, **5**, 633–4

D'Angelo N and Merlino R L 1986 *IEEE Trans. Plasma Sci.*, **PS-14**(3), 285–6

Dawson J M, Kim H C, Arnush D, et al 1976 *Phys. Rev. Lett.*, **37**, 1547–50

Drummond W E and Rosenbluth M N 1962 *Phys. Fluids*, **5**(12), 1507–12

Dubouloz N, Pottelette R, Malingre M, et al 1991 *Geophys.Res.Lett.*, **18**, 155–8

Dupree T H 1972 *Phys. Fluids*, **15**(2), 334–44

Eliasson B and Shukla P K 2006 *Phys. Rep.* **42**, 225–90

Ergun R E, Carlson C W, McFadden J P, et al 1998a *Phys. Rev. Lett.*, **81**(4), 826–9

Ergun R E, Carlson C W, McFadden J P, et al 1998b *Geophys. Res. Lett.*, **25**, 2041–4

Ergun R E, Carlson C W, McFadden J P, et al 1998c *Geophys. Res. Lett.* **25**, 2025–8

Ergun R E 1999 *Plasma Phys. Control. Fusion*, **41**, A61–73

Erlandson R E and Ukhorskiy A J 2001 *J. Geophys. Res.*, **106**(A3), 3883–95

Forme F R E, Wahlund J-E, Opgenoorth H J, et al 1993 *J. Atmosph. Terres. Phys.*, **55**(4/5), 647–66

Franz J R, Kintner P M and Pickett J S 1998 *Geophys. Res. Lett.*, **25**, 1277–80

Franz J R, Kintner P M, Seyler C E, et al 2000 *Geophys. Res. Lett.*, **27**, 169–72

Gartenhaus S 1964 *Elements of Plasma Physics*, Rinehart and Winston Inc., New York

Gurnett D A, Shawhan S D, Brice N M, et al 1965 *J. Geophys. Res.*, **70**(7), 1665–88

Gurnett D A, Frank L A, and Lepping R P 1976 *J. Geophys. Res.*, **81**, 6059–71

Hooke W M, Tenney F H, Brennan M H, et al 1961 *Phys. Fluids*, **4**(9), 1131–41

Hosea J C and Sinclair 1969 *Phys. Rev. Lett.*, **23**(1), 3–7

Hosea J C and Sinclair 1970 *Phys. Fluids*, **13**(3), 701–11

Humphries(Jr.) S 1990 *Charged Particle Beams: 2. Phase space description of charged particle beams*, John Wiley and Sons

Karney C F F and Bers A 1977 *Phys. Rev. Lett.*, **39**, 550–4

Kikuchi H 1970 *Nature*, **225** 257–8

Kim S-H, Heinrich J R and Merlino R L 2008 *Planet. Space Sci.*, **56**(11), 1552–9

Kindel J M and Kennel C F 1971 *J. Geophys. Res.*, **76**(13), 3055–78

Kintner P M, Kelley M C, and Mozer F S 1978 *Geophys. Res. Lett.*, **5**, 139–142

Ma J Z G and St-Maurice J-P 2008 *J. Geophys. Res.* **113**, A05312

Ma J Z G and St-Maurice J-P 2015 *Astrophy Space Sci.* **307**, 104, 1–20

Ma J Z G and Hirose A 2009 *Phys. Scr.* **79**, 045502

Ma J Z G, St-Maurice J-P, and Hirose A 2009 *Phys. Scr.* **80**, 025501

Matsumoto H, Kojima H, Miyatake T, et al 1994 *Geophys. Res. Lett.*, **21**, 2915–8

McFadden J P, Carlson C W, Ergun R E, et al 1999 *J. Geophys. Res.*, **104**(A7), 14671–82

McFadden J P, Carlson C W, Ergun R E, et al 2003 *J. Geophys. Res.* **108**(A4), 8018

Mosier S R and Gurnett D A 1969 *Nature*, **223**, 605–6

Mottez F 2001 *Astrophys. Space Sci.*, **277**, 59–70

Mozer F S, Ergun R E, Temerin M, et al 1997 *Phys.Rev.Lett.*, **79**, 1281–4

Müller G 1974 *Plasma Phys.*, **16**, 813–22

Mursula K, Bräysy T, Niskala K, et al 2001 *J. Geophys. Res.*, **106**(A12), 29543–53

Nishida A, Hada T, Anderson K A, et al 1985 *J. Geophys. Res.*, **90**, 4453–60

Ono M, Wurden G A and Wong K L 1984 *Phys. Rev. Lett.*, **52**(1), 37–40

Papadopoulos K 1977 *Rev. Geophys. Space Phys.*, **15**, 113–27

Pickett J S, Chen L-J, Kahler S W, et al 2004 *Annales Geophysicae*, **22**, 2515–23

Pickett J S, Chen L-J, Kahler S W, et al 2005 *Nonlinear Processes in Geophys.*, **12**, 181–93

Sato N and Hatakeyama R 1985 *J. Phys. Soc. Japan*, **54**(5), 1661–4

Sawley M L and Tran M Q 1982 *Lausanne Rep.*, LRP **206**/82, 1–56

Sawley M L 1990 *Lausanne Rep.*, LRP **422**/90, 1–29

Sawley M L and Paris P J 1990 *Lausanne Rep.*, LRP **423**/90, 1–24

Sawley M L and Paris P J 1991 *J. Phys. D: Appl. Phys.*, **24**, 2135–48

Scarf F L, Frank L A, Ackerson K L, et al 1974 *Geophys. Res. Lett.*, **1**, 189–92

Schmidt G 1979 *Physics of High Temperature Plasmas* (2nd ed.), Academic Press, New York

Schunk R W and Walker J C G 1970 *Planet. Space Sci.*, **18**(11), 1535-50

Smith R L, Brice N M, Katsufrakis J, et al 1964 *Nature*, **204**, 274–275

Song B, Suszcynsky D, D'Angelo N, et al 1989 *Phys. Fluids B*, **1**(12), 2316–8

Stix T H 1957 *Phys. Rev.*, **106**(6), 1146–50

Stix T H 1958 *Phys. Fluids*, **1**(4), 308–17

St.-Maurice J P 1987 *J. Geophys. Res.*, **92**, 4533–42

St-Maurice J-P, Winkler E and Hamza A M 1994 *J. Geophys. Res.*, **99**, 19,527–48

Strozzi D J, Ram A K and Bers A 2003 *Phys. Plasmas*, **10**(7), 2722–31

Temerin M, Cerny K, Lotko W, et al 1982 *Phys. Rev. Lett.*, **48**, 1175–9

Vojko M and Dali D 1996 *IEEE trans. instrum. meas.*, **45**(2), 561–3

Vojko M, Dali D, and Jože 1994 *Sensors and actuators. A Physical*, **a42**(1/3), 465–71

Woods L C 1962 *J. Fluid Mech.*, **13**(4), 570–86

Yoshikawa S, Rothman M A, and Sinclair R M 1965 *Phys. Rev. Lett.*, **14**(7), 214–6

Weibel E S 1980 *Phys. Rev. Lett.*, **44**(6), 377–9